Supporting Information

Dihalo bismuth cations: unusual coordination properties and inverse solvent effects in Lewis acidity

Jacqueline Ramler,[a] Andreas Stoy,[d] Tobias Preitschopf,[b] Janosch Kettner,[d] Ingo Fischer,[b] Bernhard Roling,[d] Felipe Fantuzzi,[c] and Crispin Lichtenberg*[a,d]*

[a] Dr. J. Ramler, Prof. Dr. C. Lichtenberg
Institute of Inorganic Chemistry
Julius-Maximilians-University Würzburg
Am Hubland, 97074 Würzburg (Germany)

[b] T. Preitschopf, Prof. Dr. I. Fischer
Institute of Physical and Theoretical Chemistry,
Julius-Maximilians-University Würzburg,
Am Hubland, 97074 Würzburg (Germany)

[c] Prof. Dr. F. Fantuzzi
School of Physical Sciences, Ingram Building
University of Kent
Park Wood Rd, Canterbury CT2 7NH (UK)

[d] Dr. A. Stoy, J. Kettner, Prof. Dr. B. Roling, Prof. Dr. C. Lichtenberg
Department of Chemistry
Philipps-University Marburg
Hans-Meerwein-Str. 4, 35032 Marburg, (Germany)
E-mail: crispin.lichtenberg@chemie.uni-marburg.de

Table of Contents

Experimental

General considerations. All air- and moisture-sensitive manipulations were carried out using standard vacuum line Schlenk techniques or in a glovebox containing an atmosphere of purified argon. Solvents were degassed and purified according to standard laboratory procedures. NMR spectra were recorded on Bruker instruments operating at 400 or 500 MHz with respect to ^{1}H. ^{1}H and ^{13}C NMR chemical shifts are reported relative to $SiMe_4$ using the residual ^{1}H and ^{13}C chemical shifts of the solvent as a secondary standard. ^{11}B and ^{19}F NMR chemical shifts are reported relative to $BF_3 \cdot OEt_2$ and $CFCl_3$ as external standards. NMR spectra were recorded at ambient temperature (typically 23 °C), if not otherwise noted. IR spectroscopic measurements were conducted on a Bruker Alpha ATR-IR spectrometer. Elemental analyses were performed on a Leco or a Carlo Erba instrument, and the results are given in %. Single crystals suitable for X-ray diffraction analysis were coated with poly*iso*butylene or perfluorinated polyether oil in a glovebox, transferred to a nylon loop and then to the goniometer of a diffractometer equipped with a molybdenum X-ray tube ($K\alpha\lambda$ = 0.71073 Å). The data obtained were integrated with SAINT and a semi-empirical absorption correction from equivalents with SADABS was applied. The structure was solved and refined using the Bruker SHELX 2014 software package. All non-hydrogen atoms were refined with anisotropic displacement parameters. All hydrogen atoms were refined isotropically on calculated positions by using a riding model with their U_{iso} values constrained to 1.5 U_{eq} of their pivot atoms for terminal sp^3 carbon atoms and 1.2 for all other atoms. Crystallographic data have been deposited with the Cambridge Crystallographic Data Centre as supplementary publication numbers 2190606-2190609. These data can be obtained free of charge from The Cambridge Crystallographic Data Centre.

1-Cl.
$BiCl_3$ (50.0 mg, 0.16 mmol) was added to a solution of Tl[$BArF^{24}$] (0.16 g, 0.16 mmol) in pyridine (1.5 mL). The precipitate was removed by filtration and the filtrate was layered with *n*-pentane (2 mL). After 16 h at –30 °C a colorless solid was isolated by filtration and dried *in vacuo*. Yield: 0.17 g, 0.11 mmol, 70%.

^{1}H NMR (400 MHz, CD_2Cl_2): δ = 7.48 (m, 10H, *meta*-C_5H_5N), 7.55 (s, br, 4H, *para*-$BArF^{24}$), 7.72 (s, br, 8H, *ortho*-$BArF^{24}$), 7.93 (t, 5H, $^{3}J_{HH}$ = 6.1 Hz, *para*-C_5H_5N), 8.76 (d, 10H, $^{3}J_{HH}$ = 4.8 Hz, *ortho*-C_5H_5N) ppm.
^{11}B NMR (128 MHz, CD_2Cl_2): δ = −6.6 (s, $BArF^{24}$) ppm.
^{13}C NMR (100 MHz, CD_2Cl_2): δ = 117.87 (m, *para*-$C_6H_3(CF_3)_2$), 124.98 (quart, $^{3}J_{CF}$ = 272.2 Hz, CF_3), 125.96 (s, *meta*-C_5H_5N), 129.27 (quartquart, $^{2}J_{CF}$ = 31.6 Hz, $^{4}J_{CF}$ = 2.7 Hz, *meta*-(3,5-$C_6H_3(CF_3)_2$), 135.18 (s, br, *ortho*-$C_6H_3(CF_3)_2$), 139.77 (s, *para*-C_5H_5N), 147.84 (s, *ortho*-C_5H_5N), 162.20 (quart, $^{1}J_{BC}$ = 49.9 Hz, *ipso*-$C_6H_3(CF_3)_2$) ppm.
^{19}F NMR (376 MHz, CD_2Cl_2): δ = −62.9 (s, CF_3) ppm.

Elemental analysis: Anal. calc. for $C_{32}H_{12}BBiCl_2F_{24}(py)_{4.5}$ (1497.67 g · mol^{-1}): C 43.67, H 2.32, N 4.20; found: C 43.35, H 2.52, N 4.36.[i]

[i] Compounds **1-X** (X = Cl, Br, I) and **1*-Br** are susceptible to partial loss of pyridine, when dried in vacuo for prolonged periods of time (> 3 h).

1-Br. $BiBr_3$ (50.0 mg, 0.11 mmol) was added to a solution of $Tl[BArF^{24}]$ (0.11 g, 0.11 mmol) in pyridine (1.5 mL). The precipitate was removed by filtration and the filtrate was layered with *n*-pentane (2 mL). After 16 h at –30 °C a colorless solid was isolated by filtration and dried *in vacuo*. Yield: 0.12 g, 98.3 µmol, 86%.

^{1}H NMR (400 MHz, CD_2Cl_2): δ = 7.45 (m, 10H, *meta*-C_5H_5N), 7.55 (s, br, 4H, *para*-$BArF^{24}$), 7.72 (s, br, 8H, *ortho*-$BArF^{24}$), 7.91 (t, 5H, $^3J_{HH}$ = 6.1 Hz, *para*-C_5H_5N), 8.95 (d, 10H, $^3J_{HH}$ = 4.9 Hz, *ortho*-C_5H_5N) ppm.
^{11}B NMR (128 MHz, CD_2Cl_2): δ = −6.6 (s, $BArF^{24}$) ppm.
^{13}C NMR (100 MHz, CD_2Cl_2): δ = 117.82 (m, *para*-$C_6H_3(CF_3)_2$), 124.95 (quart, $^3J_{CF}$ = 271.8 Hz, CF_3), 126.37 (s, *meta*-C_5H_5N), 129.27 (quartquart, $^2J_{CF}$ = 31.5 Hz, $^4J_{CF}$ = 2.8 Hz, *meta*-(3,5-$C_6H_3(CF_3)_2$), 135.15 (s, br, *ortho*-$C_6H_3(CF_3)_2$), 140.10 (s, *para*-C_5H_5N), 148.42 (s, *ortho*-C_5H_5N), 162.11 (quart, $^1J_{BC}$ = 48.9 Hz, *ipso*-$C_6H_3(CF_3)_2$) ppm.
^{19}F NMR (376 MHz, CD_2Cl_2): δ = −62.9 (s, CF_3) ppm.

Elemental analysis: Anal. calc. for $C_{32}H_{12}BBiBr_2F_{24}(py)_{4.0}$ (1546.42 g · mol^{-1}): C 40.34, H 2.08, N 3.62; found: C 40.69, H 1.82, N 3.50.[i]

1-I. BiI_3 (50.0 mg, 84.7 µmol) was added to a solution of $Tl[BArF^{24}]$ (87.5 mg, 84.7 µmol) in pyridine (1.0 mL). The precipitate was removed by filtration and the filtrate was layered with *n*-pentane (2 mL). After 16 h at –30 °C an orange solid was isolated by filtration and dried *in vacuo*. Yield: 0.12 g, 72.0 µmol, 85%.

^{1}H NMR (400 MHz, CD_2Cl_2): δ = 7.36 (m, 10H, *meta*-C_5H_5N), 7.55 (s, br, 4H, *para*-$BArF^{24}$), 7.72 (s, br, 8H, *ortho*-$BArF^{24}$), 7.87 (t, 5H, $^3J_{HH}$ = 7.7 Hz, *para*-C_5H_5N), 8.88 (d, 10H, $^3J_{HH}$ = 3.4 Hz, *ortho*-C_5H_5N) ppm.
^{11}B NMR (128 MHz, CD_2Cl_2): δ = −6.6 (s, $BArF^{24}$) ppm.
^{13}C NMR (100 MHz, CD_2Cl_2): δ = 117.86 (m, *para*-$C_6H_3(CF_3)_2$), 124.97 (quart, $^3J_{CF}$ = 272.5 Hz, CF_3), 126.05 (s, *meta*-C_5H_5N), 129.25 (quartquart, $^4J_{CF}$ = 2.3 Hz, $^2J_{CF}$ = 29.2 Hz, *meta*-(3,5-$C_6H_3(CF_3)_2$), 135.18 (s, br, *ortho*-$C_6H_3(CF_3)_2$), 139.02 (s, *para*-C_5H_5N), 150.41 (s, *ortho*-C_5H_5N), 162.64 (quart, $^1J_{BC}$ = 50.6 Hz, *ipso*-$C_6H_3(CF_3)_2$) ppm.
^{19}F NMR (376 MHz, CD_2Cl_2): δ = −62.9 (s, CF_3) ppm.

Elemental analysis: Anal. calc. (%) for $C_{32}H_{12}BBiI_2F_{24}(py)_{3.5}$ (1602.87 g · mol^{-1}): C 37.09, H 1.86, N 3.06; found: C 37.33, H 2.12, N 2.91.[i]

$[BiCl_3(py)_4]$. Compound $[BiCl_3(py)_4]$ was synthesized according to the literature.[1]

$[BiBr_2(py)_5][BiBr_4(py)_2]\cdot[BiBr_3(py)_2]_2\cdot(py)_n$ (1*-Br). Single crystals of **1*-Br** were obtained by slow diffusion of hexane into a saturated solution of $BiBr_3$ (43 mg, 95 µmol) in pyridine at ambient temperature overnight. This way colorless blocks of **1*-Br** formed on the vessel walls. The supernatant was decanted. The solid was washed with n-hexane (3 × 2 mL) and briefly dried in vacuo (so that the crystalline material would turn dull).
Yield (n = 2): 54 mg, 19 µmol, 80%

Elemental analysis: Anal. calc. (%) for $Bi_4Br_{12}(py)_{13}$ (2823.10 g · mol^{-1}): C 27.65, H 2.32, N 6.45; found: C 27.95, H 2.51, N 6.52.[ii]

IR (ATR, cm^{-1}) ν: 3054 (m), 1629 (w), 1594 (s), 1483 (w), 1441 (s), 1355 (w), 1236 (s), 1209 (w), 1151 (s), 1061 (w), 1032 (s), 1003 (s), 875 (w), 745 (w), 690 (s), 620 (w), 416 (w).

[ii] The amount of pyridine in samples of **1*-Br** depends on the time the sample is exposed to reduced pressure. When dried for extended periods of time, the material turns dull, indicating loss of lattice-bound solvent molecules.

Single Crystal X-ray Diffraction Analysis

The molecular structure of **1-Cl** in the solid state has been discussed in the main text. Additional bond length and angles are given in Figure S1.

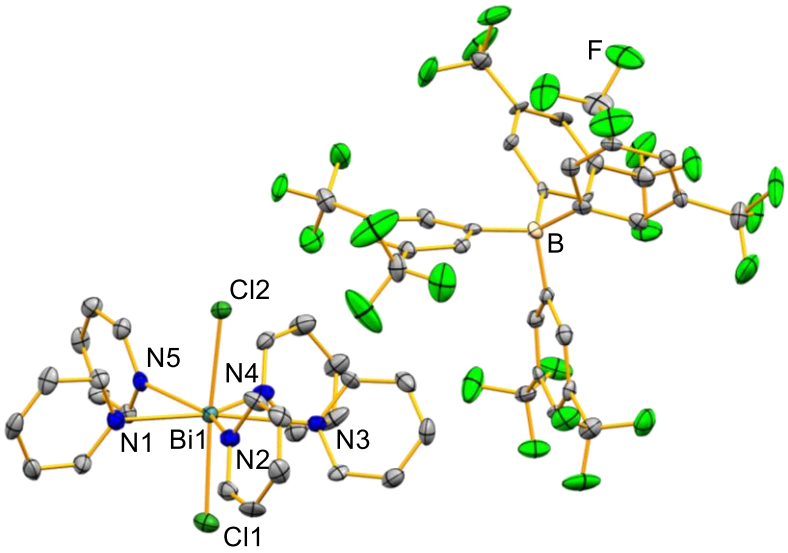

Figure S1. Molecular structure of **1-Cl** in the solid state. Displacement ellipsoids are shown at the 50% probability level. Hydrogen atoms and split positions are omitted for clarity. Selected bond lengths (Å) and angles (°): Bi1–Cl1, 2.666(2); Bi1–Cl2, 2.626(2); Bi1–N1, 2.539(7); Bi1–N2, 2.606(6); Bi1–N3, 2.611(6); Bi1–N4, 2.621(7); Bi1–N5, 2.547(7); Cl1–Bi1–Cl2, 174.35(7); N1–Bi–N2, 73.7(2); N1–Bi1–N3, 143.6(2); N1–Bi1–N4, 146.1(2); N1–Bi1–N5, 75.2(2); N2–Bi1–N3, 69.9(2); N2–Bi1–N4, 140.2(2); N2–Bi1–N5, 148.0(2); N3–Bi1–N4, 70.3(2); N3–Bi1–N5, 140.9(2); N4–Bi1–N5, 71.0(2); Cl1–Bi1–N1, 91.00(16); Cl1–Bi1–N2, 89.92(15); Cl1–Bi1–N3, 88.78(15); Cl1–Bi1–N4, 91.09(16); Cl1–Bi1–N5, 97.62(16); Cl2–Bi1–N1, 90.90(16); Cl2–Bi1–N2, 85.51(15); Cl2–Bi1–N3, 86.53(15); Cl2–Bi1–N4, 90.30(16); Cl2–Bi1–N5, 88.01.

Compound [$BiBr_2(py)_5$][BArF] (1-Br). As described in the main text, crystallographic data for compound [$BiBr_2(py)_5$][BArF] (**1-Br**) does not allow the discussion of bond lengths and angles, and the data only serves as proof of connectivity. This is due to twinning, for which suitable models could not be established and significant residual positive electron density, which was observed close to the heavy atoms Bi1 (shown) and Bi2 (not shown), which is likely due to absorption and truncation effects. A graphic representation of the molecular structure, which stands in analogy to **1-Cl**, is shown in Figure S2 (orthorhombic space group $Pca2_1$ with Z = 4). The asymmetric unit contains two formula units of **1-Br**, only one of which is shown in Figure S2.

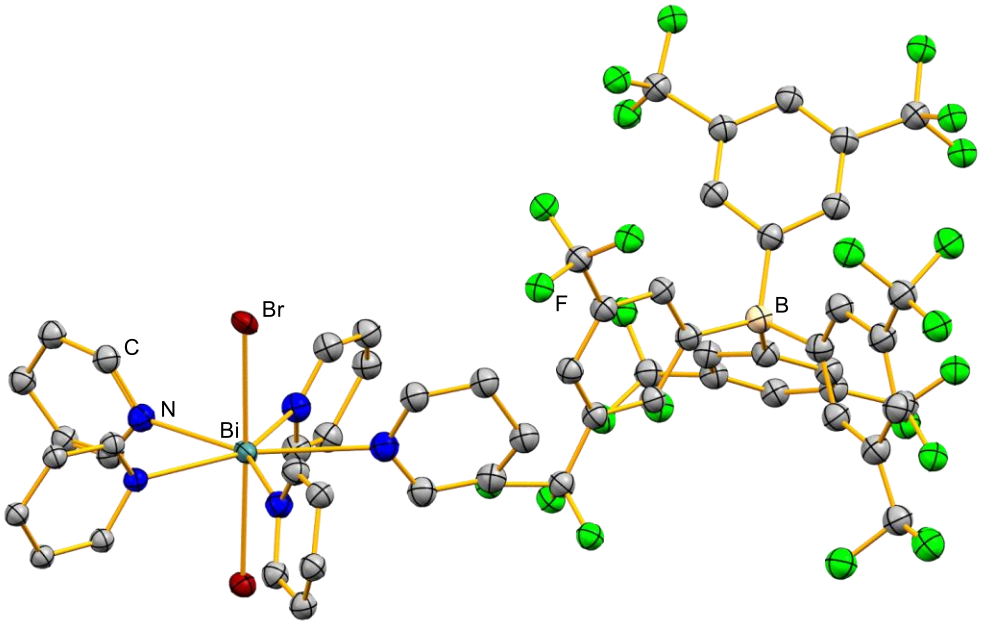

Figure S2. Molecular structure of **1-Br** in the solid state. Hydrogen atoms and second formula unit are omitted for clarity. Unit cell parameters: a = 31.3492(16) Å; b = 16.8635(10) Å; c = 24.0725(15) Å; α = 90°; β = 90°; γ = 90°; V = 12726.1(13) Å^3.

Compound [BiI$_2$(py)$_5$][BArF] (1-I). As described in the main text, crystallographic data for compound [BiI$_2$(py)$_5$][BArF] (**1-I**) is not sufficient for a detailed discussion of bonding parameters, and the data only serves as proof of connectivity. A graphic representation of the molecular structure, which stands in analogy to **1-Cl**, is shown in Figure S3 (monoclinic space group *Cc* with *Z* = 4). The asymmetric unit contains two formula units of **1-I**, only one of which is shown in Figure S3.

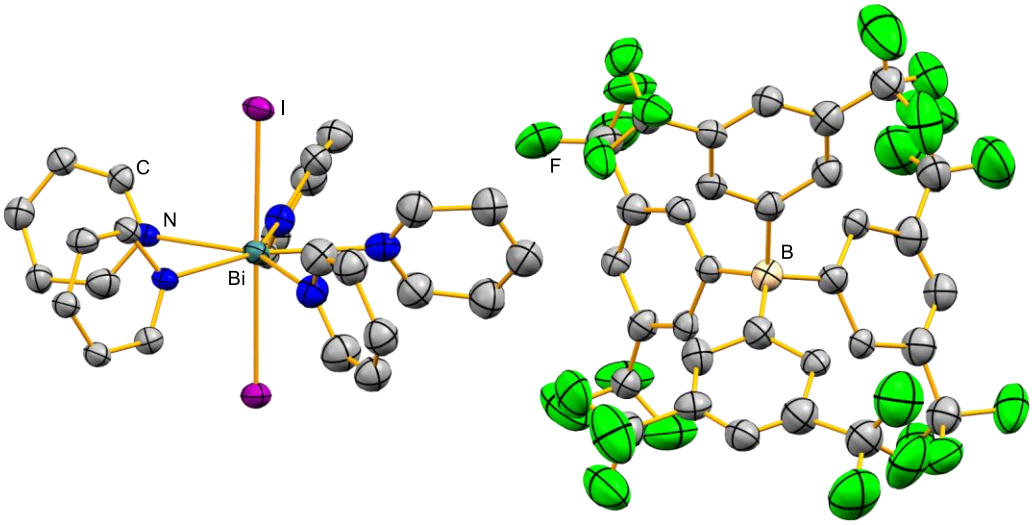

Figure S3. Molecular structure of **1-I** in the solid state. Hydrogen atoms and second formula unit are omitted for clarity. Unit cell parameters: a = 21.400(5) Å; b = 13.035(5) Å; c = 46.098(10) Å; α = 90°; β = 96.785(14)°; γ = 90°; V = 12858(6) Å^3.

Compound $[BiBr_2(py)_5][BiBr_4(py)_2]$ (1*-Br). As described in the main text, crystallographic data for compound $[BiBr_2(py)_5][BiBr_4(py)_2]$ (**1*-Br**) does not allow the discussion of bond lengths and angles. The data only serves as proof of connectivity. This fact is most likely due to the overall insufficient quality of the single crystals that were obtained. Due to the bad quality, residual positive electron density and numerous intensity outliners are present. A graphic representation of the molecular structure, which stands in analogy to **1-Br**, is shown in Figure S4 (trigonal space group *P-1* with $Z = 2$). The asymmetric unit contains one pyridine molecule and two co-crystalized $BiBr_3(py)_2$ units that were omitted for clarity.

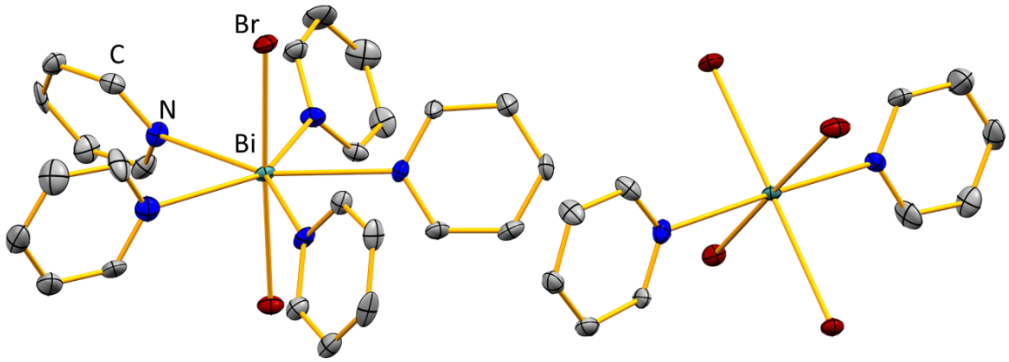

Figure S4. Molecular structure of **1*-Br** in the solid state. Hydrogen atoms, one pyridine molecule and both of the co-crystalized $BiBr_3(py)_2$ units were omitted for clarity. Unit cell parameters: a = 12.8918(16) Å; b = 13.878(2) Å; c = 19.038(4) Å; α = 98.159(14)°; β = 90.508(11)°; γ = 111.216(8)°; V = 3136.6(9) $Å^3$.

The molecular structure of **2-Cl** in the solid state is discussed further below. Additional bond lengths and angles are given in Figure S5.

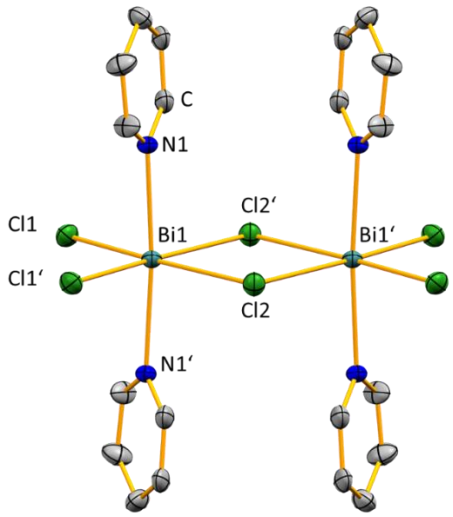

Figure S5. Molecular structure of **2-Cl** in the solid state. Hydrogen atoms were omitted for clarity. Selected bond lengths (Å) and angles (°): Bi1–Bi1', 4.269; Bi1–Cl1, 2.553(3); Bi1–Cl2, 2.898(3); Bi1–N1, 2.528(11); Bi1–N1', 2.528(11); Cl1–Bi1–Cl1', 93.33(17); Cl1–Bi1–Cl2', 90.78(11); Cl2–Bi1–Cl2', 85.11(14); Cl2–Bi1–Cl1', 90.78(11); Cl1–Bi1–N1, 88.4(3); Cl1'–Bi1–N1, 88.7(3); Cl2–Bi1–N1, 91.4(3); Cl2'–Bi1–N1, 91.8(3).

The molecular structure of **2-Br** in the solid state is discussed further below. Additional bond lengths and angles are given in Figure S6.

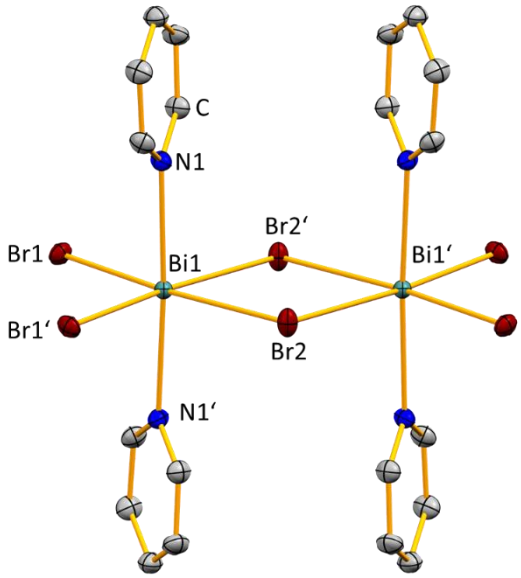

Figure S6. Molecular structure of **2-Br** in the solid state. Hydrogen atoms were omitted for clarity. Selected bond lengths (Å) and angles (°): Bi1–Bi1', 4.403; Bi1–Br1, 2.6994(4); Bi1–Br2, 3.0149(4); Bi1–N1, 2.508(2); Bi1–N1', 2.508(2); Br1–Bi1–Br1', 95.050(17); Br1–Bi1–Br2', 89.404(14); Br2–Bi1–Br2', 86.197(15); Br2–Bi1–Br1', 89.404(14); Br1–Bi1–N1, 88.04(6); Br1'–Bi1–N1, 89.82(6); Br2–Bi1–N1, 90.25(6); Br2'–Bi1–N1, 92.05(6).

The molecular structure of **2-I** in the solid state is discussed further below. Additional bond lengths and angles are given in Figure S7.

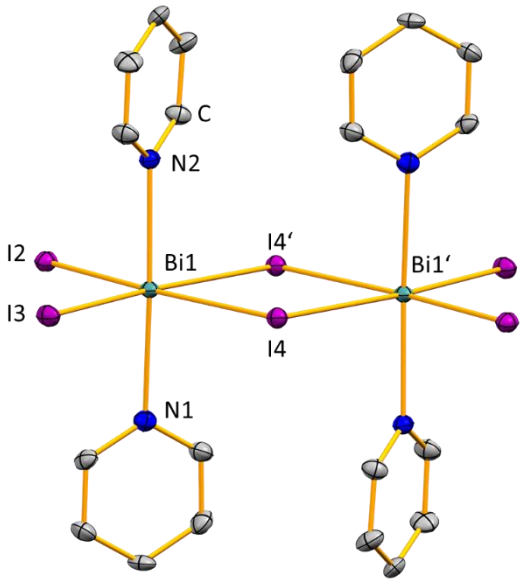

Figure S7. Molecular structure of **2-I** in the solid state. Hydrogen atoms were omitted for clarity. Selected bond lengths (Å) and angles (°): Bi1–Bi1', 4.804; Bi1–I2, 2.8982(7); Bi1–I3, 2.8959(7); Bi1–I4', 3.2794(7); Bi1–I4, 3.2623(7); Bi1–N2, 2.522(7); Bi1–N1, 2.573(7); I2–Bi1–I3, 96.09(2); I2–Bi1–I4', 89.33(2); I4'–Bi1–I4, 85.492(19); I4–Bi1–I3, 89.09(2); I2–Bi1–N2, 88.28(15); I3–Bi1–N2, 90.90(15); I4'–Bi1–N2, 90.25(16); I4–Bi1–N2, 91.32(15); I2–Bi1–N1, 88.24(15); I3–Bi1–N1, 90.21(15); I4'–Bi1–N1, 88.97(15); I4–Bi1–N1, 92.08(15).

Discussion of the Molecular Structures of $[BiX_3(py)_2]_2$ (X = Cl, Br, I). In the course of this work small amounts of $[BiCl_3(py)_2]_2$ (**2-Cl**), $[BiBr_3(py)_2]_2$ (**2-Br**) and $[BiI_3(py)_2]_2$ (**2-I**), which were suitable for single-crystal X-ray diffraction analysis, were obtained (Figure S5, Figure S6 and Figure S7). **2-Cl** crystallized in the monoclinic space group *C*2/*m* with *Z* = 2, whereas **2-Br** crystallized in the monoclinic space group *I*2/*m* with *Z* = 4, and **2-I** crystallized in the triclinic space group *P-1* with *Z* = 1. In the solid state, **2-Cl**, **2-Br** and **2-I** form dinuclear structures, in which two halide ligands adopt bridging coordination modes, which is in accordance to the analogue antimony compound.[2] The bismuth atoms possess octahedral coordination geometries with four equatorial halogen atoms and two pyridine ligands in apical positions (N1−Bi1−N1'/N2: 175.2° (**2-Cl**), 177.86° (**2-Br)**, 176.52° (**2-I)**). The terminal Bi−X bond lengths (2.55 Å (**2-Cl**), 2.70 Å (**2-Br**), 2.90 Å (**2-I**)) are considerably shorter than the Bi−X distances of bridging moieties (2.90 Å (**2-Cl**), 3.01 Å (**2-Br**), 3.28 Å (**2-I**)). These Bi−X bond lengths are in the range of reported Bi−X bond distances for bridging and terminal halogen ligands.[3,4,5] However, it may be noted that only a very limited number of species $[BiX_3L_2]_2$ with L *trans* to each other are

described in the literature.[4,5,6] The Bi−N bond lengths (2.53 Å (**2-Cl**), 2.51 Å (**2-Br**) and 2.55 Å (**2-I**)) are in the range of Bi–N distances observed in other Lewis acid/base adducts with N-donor ligands.[5,7] A bismuth-bismuth interaction is not observed based on distance criteria (the Bi···Bi distance (4.27 Å (**2-Cl**), 4.40 Å (**2-Br**) and 4.80 Å (**2-I**)) exceeds the sum of the van der Waals radii (4.14 Å) by 3%, 6% and 16%). π-Stacking between pyridine ligands of neighboring formula units is present, resulting in a two-dimensional coordination polymer in the solid state. In summary, most of the significant structural parameters of **2-X** (X = Cl, Br, I) are very similar to each other. As one exception, the exocyclic angles X–Bi1–X may be noted, which slightly increase from X = Cl to X = I (Cl1–Bi1–Cl1', 93.33(17), Br1–Bi1–Br1', 95.050(17) and I1–Bi1–I2, 96.09(2)), most likely a result of the increasing van der Waals radii of the bismuth bound halogens. Interestingly, another pyridine adduct of $BiCl_3$, namely $BiCl_3(py)_4$, has been described in the literature along with its solid-state structure.[1] As detailed below, DFT calculations suggest that dinuclear $[BiCl_3(py)_2]_2$ is thermodynamically slightly disfavored at 298 K (but favored at higher temperatures). Crystallization attempts commonly gave $BiCl_3(py)_4$ in our hands with a few exceptions, when $[BiCl_3(py)_2]_2$ was obtained, reflecting the complexity of the system.

Raman Spectroscopy

All Raman spectra were recorded with a custom-made spectrometer using a 250 mm monochromator equipped with a 1200 lines/mm grating; the exit slit had been removed and a Peltier-cooled CMOS camera (5544 x 3694 pixels) was attached to the spectrometer. An edge filter was set in front of the entrance slit and a slit width of 10 µm was used. All measurements were performed under inert gas atmosphere (Ar) at room temperature in the spectral range of 50-1100 cm^{-1}. The excitation wavelength of 532 nm was provided by an optically pumped semiconductor laser (OPSL) with a power of approximately 100 mW at the sample. Accumulation times were 30 s for $BiCl_3$, 45 s for $[BiCl_3(py)_4]$, and 10 min for **1-Cl**.

For $[BiCl_3(py)_4]$ and **1-Cl**, intrinsic fluorescence background was subtracted by using the second-order derivative method as implemented in the *OriginPro 2019b* (64-bit) data analysis software. The quality of the corresponding spectra was improved by digital Savitzky-Golay filtering.

The vibrational bands of the spectra were assigned based on harmonic Raman frequency calculations performed at the DFT/B3LYP level of theory with 6–31G(d,p) [H, B, C, N, F, Cl] and LANL2DZ [Bi] basis sets employing the *Gaussian16* computational chemistry software.[8] The computed Raman scattering activity coefficients S_j were converted into theoretical Raman intensities I_j according to equation (1):[9,10]

$$I_j = C \cdot \left(\tilde{\nu}_0 - \tilde{\nu}_j\right)^4 \cdot \tilde{\nu}_j^{-1} \cdot B_j^{-1} \cdot S_j \qquad (1)$$

where C is a constant, $\tilde{\nu}_0$ is the exciting frequency, $\tilde{\nu}_j$ is the frequency of the normal mode Q_j, and B_j is a temperature factor, which accounts for the intensity contribution of excited vibrational states. In a first approximation, this factor was set to 1 in accordance with the literature.[9] The computed frequencies $\tilde{\nu}_j$ were scaled with an empirical factor (0.90 for $BiCl_3$, 0.985 for $[BiCl_3(py)_4]$, and 0.98 for **1-Cl**). To simplify comparison with the experimental spectra, the resulting stick spectra were finally convolved with a Gaussian-shaped function with a full width at half maximum (FHWM) of 8 cm^{-1}. Figure S8 presents the experimental Raman spectra of $BiCl_3$, $[BiCl_3(py)_4]$, and **1-Cl** (black lines) along with harmonic Raman frequency computations (blue lines).

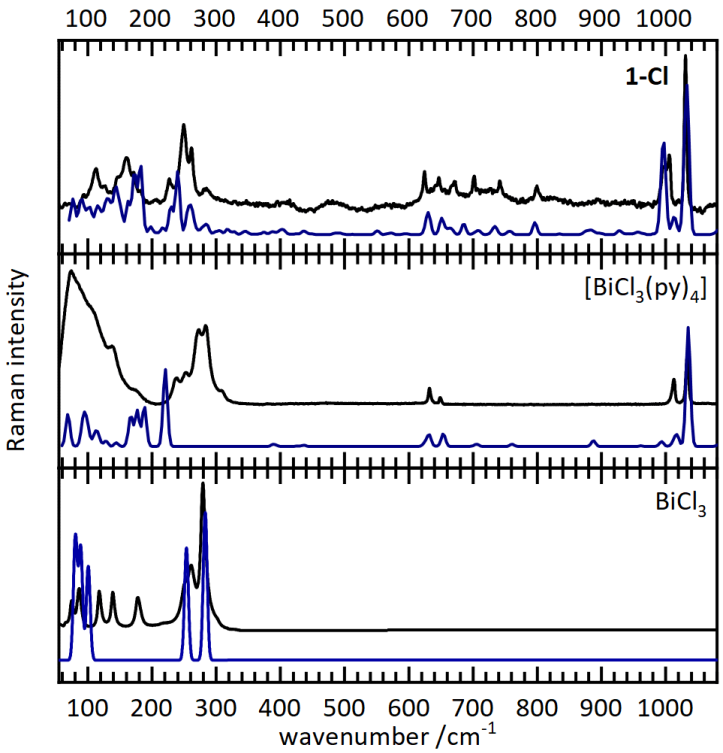

Figure S8. Comparison of the experimental Raman spectra of $BiCl_3$, $[BiCl_3(py)_4]$, and **1-Cl** (black lines) with harmonic Raman frequency computations at the DFT/B3LYP level of theory with 6–31G(d,p) [H, B, C, N, F, Cl] and LANL2DZ [Bi] basis sets employing the Gaussian16 computational chemistry software (blue lines).

$BiCl_3$. The most intense feature at 279 cm^{-1} of the experimental spectrum of $BiCl_3$ (bottom trace) is assigned to the symmetric stretching vibration. This is in excellent agreement with the wavenumber of 280 cm^{-1} observed in previous Raman experiments of $BiCl_3$.[11,12] Moreover, the two asymmetric stretching modes at 261 cm^{-1} and at 252 cm^{-1} match the reported wavenumbers very well.[11,12] Interestingly, three signals of medium intensity and one small signal between 120-230 cm^{-1} are not predicted by the computations. However, these bands were absent in a previous Raman spectrum of $BiCl_3$ in the gas-phase as well,[13] suggesting that they appear in the solid-state Raman spectrum due to long BiCl bridge stretching modes in the crystal lattice of $BiCl_3$.[11]

$[BiCl_3(py)_4]$. At higher energies, the simulated Raman spectrum of $[BiCl_3(py)_4]$ (middle trace) is in good agreement with the experimental data, as all identifiable bands at 632 cm^{-1}, 649 cm^{-1}, 1013 cm^{-1}, and 1034 cm^{-1} are predicted well in terms of energetic position and relative signal intensities. All four signals are composed of several deformation vibrations of the pyridine rings that overlap to single peaks. At lower energies, however, the computation significantly underestimates the energetic positions of several vibrational modes that overlap to a broad band with five identifiable maxima beginning at around 320 cm^{-1}. For instance, the strongest maximum at 284 cm^{-1}, corresponding to a coupled vibration with significant contributions of the BiCl symmetric stretching vibration, is predicted at 221 cm^{-1}. Yet it is noteworthy that comparing single molecule DFT calculations with experimental data of crystals in the THz region has shown to be

insufficient before.[14] This is further reflected by the very broad and unstructured band below 200 cm^{-1} in the experimental spectrum, which might be due to interactions between molecular and lattice modes in the crystal of $[BiCl_3(py)_4]$ and thus does not appear in the computed spectrum.[15] Interestingly, the computation predicts a small difference for the Bi–Cl bond length of the three Bi–Cl bonds (in agreement with single-crystal X-ray diffraction analyses).[1] In particular, equal BiCl bond lengths (2.712(8) Å) are predicted for the two axial chlorine atoms relative to the molecular plane and a slightly smaller BiCl bond length (2.710(6) Å) is predicted for the equatorial chlorine atom. This indicates small differences in the BiCl bond strengths for the equatorial and axial chlorine atoms, which is not resolved in the experimental data.

1-Cl. The experimental Raman spectrum of **1-Cl** is depicted in the top trace of Figure S8. All identifiable bands above 200 cm^{-1} match the computed vibrations well in signal intensity and energy. Due to the complex structure of the molecule, unambiguous assignment of the various signals to isolated normal modes is demanding. In particular, the vast majority of the peaks are composed of several vibrational modes that overlap to broad signals. However, according to the computation, the strong signal at 249 cm^{-1} is due to a single normal mode which shows significant contributions of a BiCl symmetric stretching vibration. The wavenumber is in good agreement with the computation (239 cm^{-1}). Below 200 cm^{-1}, the computed band positions differ significantly from the experimental data. Again, this might indicate interactions with lattice modes in the crystal.[15]

Figure S9 shows a zoom-in on the 180-340 cm^{-1} region of the Raman spectra of $BiCl_3$, $[BiCl_3(py)_4]$, and **1-Cl**.

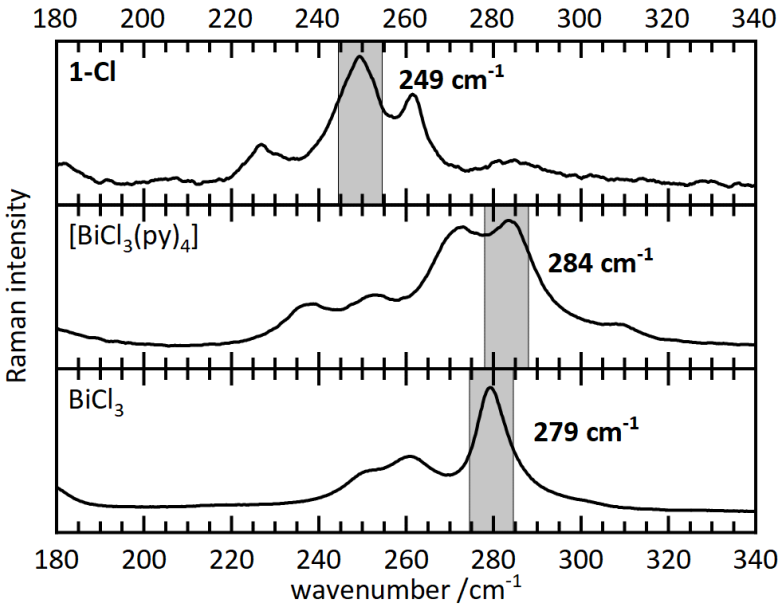

Figure S9. Zoom-in on the 180-340 cm^{-1} region of the Raman spectra of $BiCl_3$, $[BiCl_3(py)_4]$, and **1-Cl**. Bands with relevant contributions by BiCl symmetric stretching vibrations are highlighted in grey.

Conductivity measurements

Ionic conductivity measurements were carried out using a closed TSC70 liquid sample cell with a Microcell HC cell stand (rhd instruments). The cell consisted of a PEEK crucible, which was filled with 70 µL of the solution, and of two polished platinum electrodes. The impedance measurements were conducted in a frequency range from 100 kHz to 1 Hz with an ac voltage of 10 mV_{rms} by means of an Alpha-A impedance analyzer (Novocontrol Technologies) equipped with a ZG2 interface. The temperature was set to 25 °C by means of an Eurotherm 2416 temperature controller (accuracy ±0.1 °C). The software RelaxIS (rhd instruments) was used for the analysis of the impedance spectra. The equivalent circuit used for fitting the spectra consisted of a resistance in series to a constant phase element (CPE). In the case of one sample with a low ionic conductivity, an additional CPE was placed in parallel to the resistance. The resistance and the optional parallel CPE describe the bulk ion dynamics and transport in the electrolyte, while the serial CPE accounts for electrode polarization due to double layer formation. The experiments were carried out in dried and degassed solvents.
With the obtained ionic resistance (R), the ionic conductivity (σ) was calculated by using equation (2).

$$\sigma = R \cdot \frac{d}{A} \tag{2}$$

The cell constant $\left(\frac{d}{A}\right)$ of the liquid sample cell was determined by means of a 0.1 mol/L KCl standard solution (HANNA instruments) with known ionic conductivity at 25 °C.

As a suitable concentration for the BiX_3-species in solution, a value of approx. 0.1 mol/L was chosen that is frequently used in synthetic chemistry at lab scale. The exact concentrations are noted in Table S1.

Table S1. Concentrations [mol/L] of $BiCl_3$, $BiBr_3$ and BiI_3 solutions in pyridine, THF and MeCN, respectively, which were used for conductivity measurements.

Entry	solvent	$BiCl_3$	$BiBr_3$	BiI_3
1	pyridine	0.1136	0.1114	0.0565[a]
2	THF	0.0974	0.1042	0.0575[a]
3	MeCN	0.1070	0.1044	-[b]

[a] Due to the poor solubility of BiI_3 in pyridine and THF, a concentration of approx. 0.05 mol/L was targeted.
[b] The solubility of BiI_3 in acetonitrile was too low to allow conductivity measurements in the targeted concentration range.

To determine the degree of dissociation of the BiX_3-species in solution, the *Stokes-Einstein* relation (3) was used to calculate the diffusion coefficients of the anions and cations in solution; using their *van der Waals* radii approximated *via* the solid-state structure of **1*-Br** (see Figure S4), and considering the viscosity of the solvents ($\eta_{pyridine} = 8.79 \cdot 10^{-4}$ Pa·s, $\eta_{THF} = 4.60 \cdot 10^{-4}$ Pa·s, $\eta_{MeCN} = 3.34 \cdot 10^{-4}$ Pa·s).

$$D_i = \frac{k_B T}{6\pi\eta r_i} \tag{3}$$

These values were then inserted into the *Nernst-Einstein* relation (4) to estimate the maximum expected conductivity of the BiX_3-solution, where $z_i = 1$ according to the assumption that the reaction $2\ BiX_3 \rightarrow [BiX_2(L)_n][BiX_4(L)_m]$ is the dominating source of ionic species (*vide infra*).

$$\sigma = \frac{z_i^2 F^2}{RT} c_{calculated}(D_+ + D_-) \quad (4)$$

This way, the degree of dissociation can be determined by dividing the calculated concentration of conductive material, that is necessary to explain the observed conductivity, by the known concentration of BiX_3 (X = Cl, Br, I) in the corresponding solvent (equation 5).

$$degree\ of\ dissociation\ [\%] = \frac{c_{calculated}}{c_{prepared}} * 100 \quad (5)$$

In all cases, only the simple disproportionation of $2\ BiX_3 \rightarrow [BiX_2(L)_n][BiX_4(L)_m]$ was considered for the calculations (L = solvent molecule). The formation of bismuth-cations with higher charges (of up to +3) or higher nuclearity cannot be completely ruled out, but was not taken into account, since it is expected to be of minor relevance compared to the formation of monovalent ions. The appearance of species with a higher charge would be expected to increase the Lewis acidity of "BiX_3 solutions" even more than the appearance of singly charged species. The measured conductivities and calculated dissociation numbers are summarized in Table S2.

Table S2. Measured conductivities and calculated degrees of dissociation of BiX_3 (X = Cl, Br, I) in pyridine, THF and MeCN.[a]

solvent		**$BiCl_3$**	**$BiBr_3$**	**BiI_3**
pyridine	conductivity [S/m]	$1.7990 \cdot 10^{-2}$	$2.4100 \cdot 10^{-2}$	$2.4180 \cdot 10^{-2}$
	dissociation [%]	10.1	13.9	27.5
THF	conductivity [S/m]	$1.650 \cdot 10^{-3}$	$3.820 \cdot 10^{-3}$	$2.820 \cdot 10^{-3}$
	dissociation [%]	0.6	1.2	1.6
MeCN	conductivity [S/m]	$4.7860 \cdot 10^{-2}$	$4.7850 \cdot 10^{-2}$	-[a]
	dissociation [%]	10.9	11.2	-[a]

[a] The solubility of BiI_3 in acetonitrile was too low to allow conductivity measurements.

To our surprise, dissociation degrees of up to 27.5% can be observed for a BiI_3 solution in pyridine (when considering the aforementioned assumptions). The degree of dissociation increases for every solvent in the order Cl<Br<I, which was ascribed to the general trend within the periodic table of the elements, according to which Bi-X bond dissociation energies decreases with increasing atomic number of X. When comparing the solvents investigated in this study, it is apparent that the degree of dissociation is smallest in THF, presumably due to the lowest donor capabilities of THF, when compared to pyridine or acetonitrile. Unfortunately, the solubility of BiI_3 in acetonitrile was too low to allow conductivity measurements in the targeted concentration range.

These findings are especially interesting from a synthetic chemist's point of view, that in some cases, the observed reaction patterns may originate rather from the *in situ* generated bismuth cations than from the neutral BiX_3 species, when using bismuth halides as Lewis acid catalysts.

To further rule out any errors that may result from impurities, we also determined the conductivity of the pure solvents (see Table S3). This way it was clear that at least two orders of magnitude lie between the conductivity of the corresponding BiX_3-solution and that of the pure solvent, underlining the fact that the observed conductivities must originate from Bi-containing ions in solution.

Table S3. Determined conductivities of the pure solvents.

	pyridine	**THF**	**MeCN**
conductivity [S/m]	$4.3 \cdot 10^{-4}$	$3 \cdot 10^{-5}$	$1.6 \cdot 10^{-4}$

Gutmann-Beckett Method

In order to further address the Lewis acidity of the observed bismuth cations in solution, we performed a series of ^{31}P NMR measurements to quantify the solvent induced disproportionation of BiX_3 (X = Cl, Br, I) in solution *via* the traditional Gutmann-Beckett (GB) and modified Gutmann-Beckett (mGB) method,[16–18] which have recently been applied for the analysis of bismuth-based Lewis acidity.[19,20] In general, it should be noted that the GB and mGB method provide an evaluation of the Lewis acidity of the compound of interest by assessing the polarizability of the E=PR_3 bond through ^{31}P NMR spectroscopic measurements (E = O (original method); S, Se (modifications)). Being solely based on NMR spectroscopy, effects such as magnetic anisotropy of the Lewis acid (or substituents R in EPR_3), as well as concentration variations or temperature deviations and even weak London dispersion interactions may influence the results.[18,21] Furthermore, steric factors must not prohibit bonding of the probe ($OPEt_3$, $SPMe_3$, $SePMe_3$) to the Lewis acid.

As exemplified by the conductivity measurements, we assumed up to 27.5% disproportionation of the BiX_3-species into the solvent-separated ion pairs. In this case we expected that the ^{31}P NMR probe is able to displace at least one solvent molecule coordinated to the *in situ* generated $[BiX_2(L)_n]^+$ cation (Scheme S1).

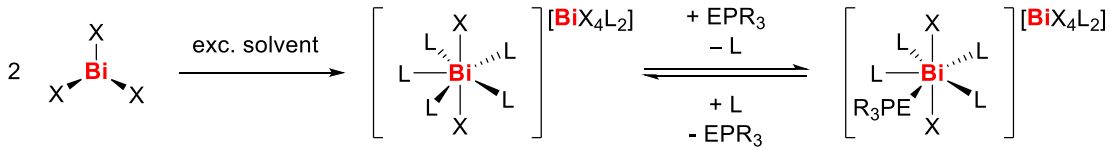

Scheme S1. Solvent-induced disproportionation of BiX_3 into the solvent separated ion pairs and displacement of one solvent molecule by the ^{31}P NMR probe $OPEt_3$, $SPMe_3$ or $SePMe_3$, respectively.

To measure accurate ^{31}P NMR shifts, three distinct methods are easily feasible: **A**: the use of deuterated solvents, so that locking and shimming is possible; **B**: the use of non-deuterated solvents along with a capillary containing a deuterated solvent, so that locking and shimming is possible; **C**: the use of non-deuterated solvents along with a capillary containing an 85% aqueous solution of H_3PO_4 as a reference.[18] In a previous publication, it could be shown that all these three methods gave identical results, when applied to identical samples.[18] In this work method **C** was used.

In the traditional GB method, a stochiometric 1:1 mixture of $OPEt_3$ and a (potential) Lewis acid is analyzed by ^{31}P NMR spectroscopy. The ^{31}P NMR shift is then inserted into equation (6) and the corresponding acceptor number (AN) is calculated.

$$AN\ (OPEt_3) = 2.21 \cdot (\ \delta(^{31}P\ NMR)_{sample}\ [ppm] - 41.0) \qquad (6)$$

As reference points, AN = 0 corresponds to $OPEt_3$ in hexane and AN = 100 equals the $OPEt_3$•$SbCl_5$ adduct in dichloroethane.[16]

The mGB method relies on the softer donors $SPMe_3$ and $SePMe_3$ to further address the soft Lewis acidic nature of the bismuth compound under investigation.[18] In analogy to the GB method, the ^{31}P NMR spectroscopy is measured and then inserted into equation (7) or (8),

$$AN\ (SPMe_3) = 6.41 \cdot (\ \delta(^{31}P\ NMR)_{sample}\ [ppm] - 29.2) \quad (7)$$

$$AN\ (SePMe_3) = 5.71 \cdot (\ \delta(^{31}P\ NMR)_{sample}\ [ppm] - 7.8) \quad (8)$$

where in this case AN = 0 equals the $EPMe_3$ probe in CH_2Cl_2 and AN = 100 corresponds to a 1:1 mixture of $EPMe_3$ with GaI_3 in CH_2Cl_2 (E = S, Se).[18]
Because of the amount of measurements, it is possible to sort the experiments in one three-dimensional matrix, or in this case, divide the results in three different tables. This way, the determined AN are summarized in Table S4, Table S5 and Table S6.

Table S4. Acceptor numbers (ANs) of a stochiometric 1:1 mixture of $BiCl_3$ with $OPEt_3$, $SPMe_3$ and $SePMe_3$ as ^{31}P NMR spectroscopic probes in the corresponding solvents.

solvent	$OPEt_3$	$SPMe_3$	$SePMe_3$
pyridine	32.8[a]	10.1	12.6
THF	47.4	18.6	28.7[a]
MeCN	66.5	56.3	82.6[a]
dichloromethane	49[b]	26[c]	14[c]

[a] After 10 min colorless to yellow powders precipitated out of solution at room temperature; [b] see literature;[20] [c] see literature.[18]

Table S5. Acceptor numbers (ANs) of a stochiometric 1:1 mixture of $BiBr_3$ with $OPEt_3$, $SPMe_3$ and $SePMe_3$ as ^{31}P NMR spectroscopic probes in the corresponding solvents.

solvent	$OPEt_3$	$SPMe_3$	$SePMe_3$
pyridine	34.3	9.7	13.1
THF	45.8	19.5	28.9[a]
MeCN	67.7	83.4[a]	77.9[a]
dichloromethane	30[b]	17[c]	11[c]

[a] After 10 min yellow to orange powders precipitated out of solution at room temperature; [b] see literature;[20] [c] see literature.[18]

Table S6. Acceptor numbers (ANs) of a stochiometric 1:1 mixture of BiI_3 with $OPEt_3$, $SPMe_3$ and $SePMe_3$ as ^{31}P NMR spectroscopic probes in the corresponding solvents.[a]

solvent	$OPEt_3$	$SPMe_3$	$SePMe_3$
pyridine	32.8	10.2	14.6
THF	43.5	15.1	25.6[b]
dichloromethane	22[c]	13[d]	10[d]

[a] The solubility of BiI_3 in acetonitrile was too low to allow measurements; [b] After 10 min a red powder precipitated out of solution at room temperature; [c] see literature;[20] [d] see literature.[18]

The conclusions that can be drawn are sorted in three groups: I.) comparing the different ^{31}P NMR spectroscopic probes with each other, II.) comparing the solvents with each other (values obtained in this and previous works[18]), and III.) drawing conclusions by comparing

different BiX_3 species with each other in the same solvent. All other conditions (type of solvent, type of BiX_3 compound or ^{31}P NMR spectroscopic probe) are kept constant.
I.) It has to be kept in mind that the acceptor numbers obtained with different probes relate to different scales and are therefore not directly comparable. Nevertheless, strong differences in acceptor numbers of different scales still hint at differences in Lewis acidity. One predominant trend is that $SPMe_3$ delivers the lowest AN throughout all measurements, except for the combination of $SPMe_3$ with $BiBr_3$ in MeCN where it has the highest observed value of all AN of 83.4 (see Table S5). The lowest determined AN of 9.7 can be found by combining $SPMe_3$ and $BiBr_3$ in pyridine. $OPEt_3$ shows tendencies to have the highest AN in THF and pyridine, whereas the AN of $SePMe_3$ lie in between those of $OPEt_3$ and $SPMe_3$. These results reflect the strong donor ability of $OPEt_3$, especially when competing with other hard donors such as the solvents used in this study.
II.) Independent of the BiX_3 species or the ^{31}P NMR spectroscopic probe, increasing ANs can be observed by changing the solvent from pyridine to THF or MeCN, respectively (see Table S4 to Table S6). This trend may be explained by the stronger donor capabilities of pyridine when compared to THF or MeCN.[22] Because pyridine is such a strong donor, the probes $OPEt_3$, $SPMe_3$, and $SePMe_3$, respectively, may be incapable of displacing the bound solvent molecules, thus leading to low ANs. This circumstance is further supported by the fact that the observed AN of mixtures consisting of BiX_3 and $SPMe_3$ or $SePMe_3$ in pyridine approach the values of pure pyridine mixed with the corresponding probe ($OPEt_3$, $SPMe_3$, and $SePMe_3$; compare to Table S7). In addition to that, it has previously been reported that higher ANs are obtained in dichloromethane for the combinations of BiX_3 with $SPMe_3$ ($BiCl_3$: AN = 26, $BiBr_3$: AN = 17, BiI_3: AN = 13) than in pyridine.[18]
III.) When comparing the $BiCl_3$, $BiBr_3$ and BiI_3 species with each other, the ANs are similar for different BiX_3 species in the same solvent and for the identical ^{31}P NMR spectroscopic probe. This suggests that whether or not a species is susceptible to ligand-induced disproportionation has a stronger effect on the AN than the degree to which ligand-induced disproportionation takes place in the absence of the probe ($OPEt_3$, $SPMe_3$, and $SePMe_3$). Moreover, it has to be kept in mind that precipitation was observed in some cases, which is more likely for species with a higher charge; i.e. the ANs measured in the solution part may not reflect the Lewis acidity of species with a higher charge that are in principle also accessible through ligand-induced disproportionation.
In addition to the aforementioned results, we performed further GB and mGB measurements of the pure solvents to establish a baseline for the observed AN of the bismuth halide species (see Table S7).

Table S7. Acceptor numbers (ANs) of the pure solvents with $OPEt_3$, $SPMe_3$ and $SePMe_3$ as ^{31}P NMR spectroscopic probes.

solvent	$OPEt_3$	$SPMe_3$	$SePMe_3$
pyridine	16.3	9.6	11.2
THF	12.1	2.4	5.5
MeCN	22.6	20.0	20.2

It should be noted that the GB and mGB method will (depending on exchange rates and differences in the chemical shifts) usually deliver an averaged AN, if more than one species containing the spectroscopic probe ($OPEt_3$, $SPMe_3$, and $SePMe_3$) is formed in solution.

Therefore, complex equilibria may not be resolved with this approach (a simple example is shown in Scheme S2).

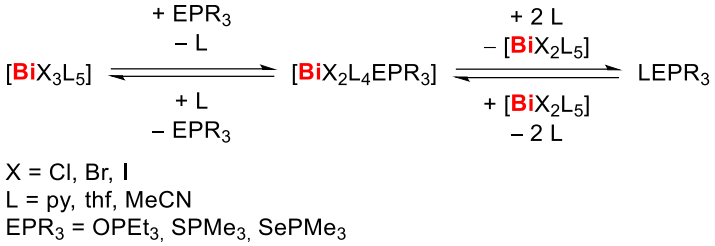

Scheme S2. Possible fast exchange events of the chemical surroundings of the ^{31}P NMR spectroscopic probes in solution.

Nevertheless, we expect in all cases, that the used ^{31}P NMR spectroscopic probes remain chemically unmodified. This circumstance is further supported by the observed ^{1}J (^{31}P^{77}Se) coupling constants of around 684 Hz that align well with literature-known values and suggest a stable probe in the case of $SePMe_3$.[23]

One drawback of this method is that it is impossible to distinguish between different bismuth cations that may form in solution. As already mentioned above, it cannot be precluded that higher Bi-cations (with charges of up to +3) are generated during the experiments. However, in this case even with higher charges on the bismuth atoms, and possibly more than one probe bound to one Bi cation, the GB and mGB method deliver averaged ANs of complex equilibria.

It must also be noted that during the measurements, in some cases, colorless, yellow to orange or red powders precipitated. This is especially true for the probe $SePMe_3$, where five out of eight times (combinations of $BiCl_3$ with THF, MeCN; $BiBr_3$ with THF, MeCN; BiI_3 with THF) bright yellow or red powders precipitated out of solution within 10 min at room temperature. In the case of trimethylphosphane sulfide only $BiBr_3$ in acetonitrile displays this behavior. In a similar fashion, combinations of triethylphosphane oxide with $BiCl_3$ or $BiBr_3$ in pyridine showed the precipitation of colorless solids. In all discussed cases however, the separate solutions of either the bismuth halide or the phosphanes are clear solutions for prolonged periods of time. Higher Bi-cations may deviate from a simple 1:1 stoichiometry (Bi:probe). This circumstance has been shown in previous works where the combination of $Bi(OTf)_3$ and $SePMe_3$ led to the formation of $[Bi(SePMe_3)_6][OTf]_3$.[18,24]

DFT Calculations

DFT calculations were performed for $[BiCl_2(py)_n]^+$ (n = 0-6) and selected $[BiCl_2(py)_n][BArF]$ and $[BiCl_3(py)_m]$ (m = 0-4) structures with the Gaussian 16, Revision C.01 program package.[8] These were done with the B3LYP[25] functional and the 6-31G(d,p)[26] (H, C, N, Cl) and LanL2DZ/ECP[27] (Bi) basis sets. The D3 version of Grimme's dispersion model with the original D3 damping function was applied.[28] Solvation corrections were incorporated with the PCM[29] solvent model and pyridine (py, ε = 12.978) as solvent. For each molecular stoichiometry, a systematic investigation was performed considering distinct initial geometries and local symmetries. All geometries reported herein are characterized as minimum energy structures as no imaginary frequencies were found. Heterolytic bond dissociation energies (BDE) were computed considering the electronic energies corrected by zero-point energy (ZPE). Gibbs free energies were calculated at a temperature of 298.15 K and a pressure of 1.00 atm. A concentration correction of $\Delta G^{0\rightarrow *}$ = RT·ln(24.46) = 1.894 kcal mol^{-1} (T = 298.15 K) was added to the free energies of all calculated species to change the 1.00 atm gas phase values to the condensed phase standard state concentration of 1.00 mol·L^{-1}. For pyridine, a standard state of 12.41 mol L^{-1} at 298.15 K was used, whereby its $\Delta G^{0\rightarrow *}$ correction is 3.386 kcal mol^{-1}. This procedure leads to a proper description of associative/dissociative steps,[30] allowing us to better estimate free energies of py addition and ligand exchange (from Cl^- to py). Finally, the Bi(*p*) character of selected molecular orbitals was computed using the orbital composition analysis with Mulliken partition as implemented in Multiwfn 3.8.[31]

Cationic species. The influence of the number of pyridine ligands on the Bi–Cl bond strengths was studied by calculating the heterolytic Bi–Cl bond dissociation energies (BDEs) of $[BiCl_3(py)_n]$ (n = 0-4; Table S8). For that, we considered distinct structures for the systems and performed the analysis on the most stable optimized geometries (see Figure S10). Our results show that the coordination of py ligands to $BiCl_3$ indeed facilitates the heterolytic Bi–Cl bond dissociation, whose BDE values range from 63.0 (n = 0) to 18.6 (n = 4) kcal mol^{-1}. These results corroborate our experimental finding that the formation of the $[BiCl_2]^+$ cation is favored by the presence of coordinating pyridine ligands. As expected, the heterolytic Bi–Cl BDE of **1-Cl**, which would lead to a dicationic $[BiCl(py)_4]^{2+}$ complex, is larger (33.8 kcal mol^{-1}) than those of the corresponding neutral $BiCl_3$ systems coordinated to pyridine ligands.

Table S8. Heterocyclic bond dissociation energies at the PCM(py)-B3LYP-D3/6-31G**;LANL2DZ(Bi) level of theory.

Dissociation	Heterolytic BDE [kcal mol^{-1}]
$BiCl_3 \rightarrow BiCl_2^+ + Cl^-$	63.0
$[BiCl_3(py)] \rightarrow [BiCl_2(py)]^+ + Cl^-$	32.5
$[BiCl_3(py)_2] \rightarrow [BiCl_2(py)_2]^+ + Cl^-$	28.7
$[BiCl_3(py)_3] \rightarrow [BiCl_2(py)_3]^+ + Cl^-$	21.3
$[BiCl_3(py)_4] \rightarrow [BiCl_2(py)_4]^+ + Cl^-$	18.6
$[BiCl_2(py)_5]^+$ (**1-Cl**)$\rightarrow [BiCl(py)_5]^{2+} + Cl^-$	33.8

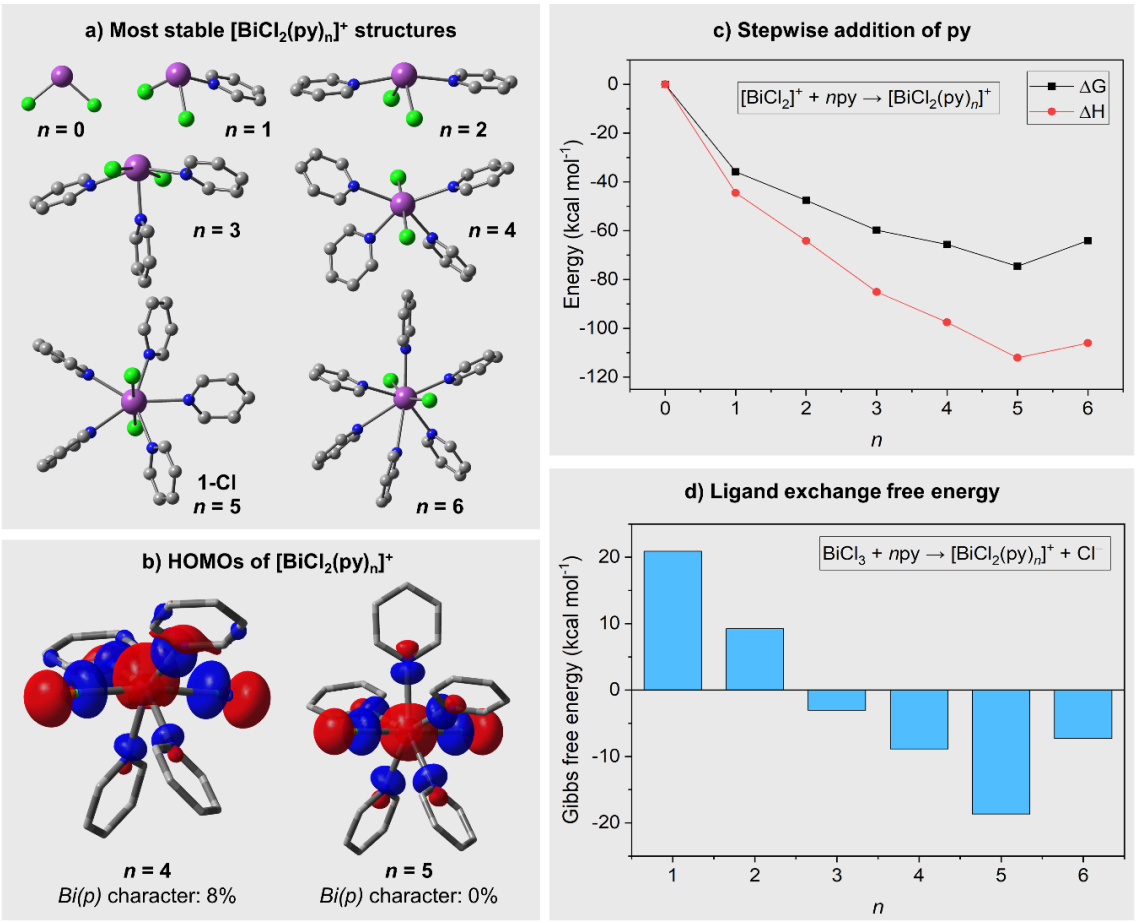

Figure S10. a) Most stable $[BiCl_2(py)_n]^+$ structures (n = 0-6) obtained herein. b) HOMOs of the distorted octahedral structure of $[BiCl_2(py)_n]^+$ (*n* = 4, left) featuring a stereochemically active Bi lone pair and the pentagonal bipyramidal structure of **1-Cl** (*n* = 5, left). Isovalues: 0.04 *a.u.* c) Energetics of the stepwise addition of *n* py to $[BiCl_2]^+$ (n = 0-6). d) Ligand exchange free energy calculated following the reaction $BiCl_3$ + *n* py → $[BiCl_2(py)_n]^+ + Cl^-$. Optimized structures and corresponding energies were obtained at the B3LYP-D3/6-31G(d,p)/LANL2DZ(Bi)+PCM(pyridine) level of theory.

With the goal of understanding the preference for the formation of **1-Cl** rather than any other $[BiCl_2(py)_n]^+$ complex, we conducted a systematic investigation on the preferred geometries and their corresponding enthalpies and free energies of formation from the isolated $[BiCl_2]^+$ and *n* pyridine ligands (*n* = 0-6, Figure S10a and S11). As the $[BArF]^-$ system is a non-coordinating anion, these investigations were carried out at the isolated cations. Additional computations explicitly including the $[BArF]^-$ counteranion have led to similar findings. The most stable $[BiCl_2(py)_n]^+$ structures obtained from our calculations are shown in Figure S10a (low-lying isomers are found in the Figure S11). The complexes for *n* = 0 and *n* = 1 have the typical angular and trigonal pyramidal structures of pnictogen systems with coordination numbers 2 and 3, respectively. For *n* = 2 (bisphenoidal), the isomer with the pyridine ligands occupying axial positions is thermodynamically favorable. In turn, for *n* = 3 (square pyramidal), *n* = 4 (distorted octahedral), *n* = 5

(pentagonal bipyramidal), and n = 6 (distorted hexagonal bipyramidal), the energetically favored isomers are those in which the chlorido ligands are situated in *trans*-positions respective to each other.

Interestingly, for n = 4 we found two structures featuring chloride ligands in *trans* positions: an octahedral structure and a more stable distorted octahedral. This latter structure has one large N–Bi–N angle (133.7°) and three small angles (73.0-76.1°) for the pyridine/chlorido ligands in the equatorial plane, which indicates a stereoactivity of the lone pair at bismuth, as also revealed by inspection of the Bi(*p*) character of its HOMO (Figure S10b). A higher energy structure featuring chloride ligands in *cis* positions and with less pronounced distortions was also found. For the *trans* structures, they are only marginally different in energy (ΔG = 1.2 kcal mol^{-1}). However, inclusion of the [BArF]$^-$ ligand led only to the optimization of the distorted octahedral structure. This suggests that the preference and access to structures with stereochemically active lone-pairs may be enhanced by the introduction of an anion.

Finally, only one stable structure for each n = 5 (pentagonal bipyramidal, **1-Cl**) and n = 6 (distorted hexagonal bipyramidal) was found. Indeed, for n = 5, all attempts to generate capped octahedron or trigonal prismatic structures failed and the structure collapsed to the global minimum **1-Cl**, which features a stereochemically inactive Bi lone pair (see Figure S10b).

Next, we compare the energies of the stepwise addition of py to $[BiCl_2]^+$ (Figure S10c, also see main part) and the ligand exchange free energy (Figure S10d) from Cl^- to pyridine. Inspection of Figure S10c reveals that the sequential addition of pyridine to $[BiCl_2]^+$ is both exothermic and exergonic up to the formation of **1-Cl** (n = 5), whereas addition of a sixth py ligand is uphill by ΔH = +10.5 kcal mol^{-1} and ΔG = +6.0 kcal mol^{-1}. Accordingly, the ligand exchange free energy values (Figure 10d) indicate that **1-Cl** is the most favorable species (ΔG = –18.7 kcal mol^{-1}) formed after the replacement of Cl^- by five pyridine ligands. These results are in excellent agreement with the experimental findings and reveal that the preference for the formation of **1-Cl** is already explained using thermodynamic reasoning.

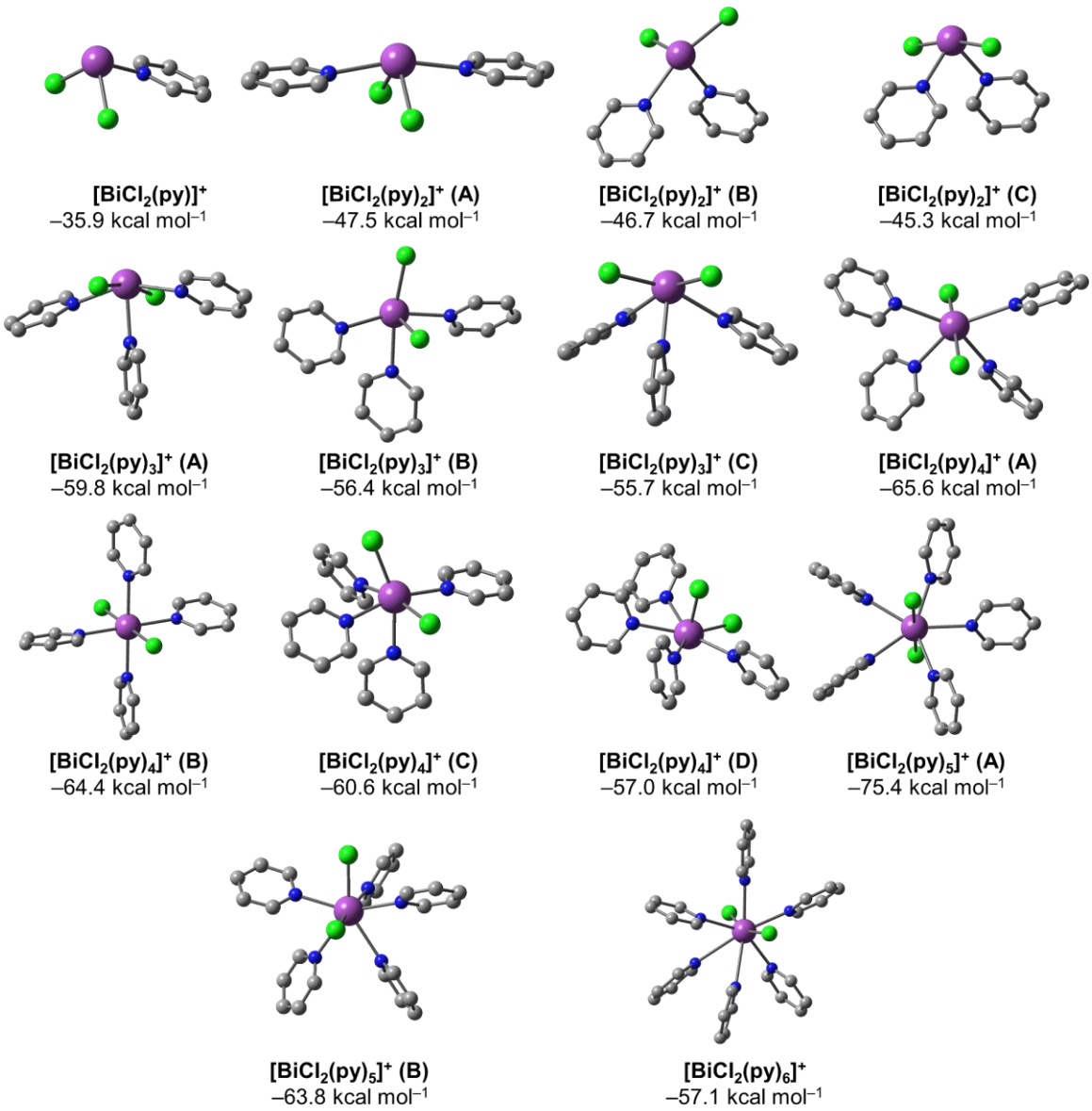

Figure S11. 3D structures of the $[BiCl_2(py)_n]^+$ systems computed herein. The free energies of the formation of each $[BiCl_2(py)_n]^+$ system from the stepwise addition of *n* py to $[BiCl_2]^+$ (n = 0-6) is also shown. Level of theory: PCM(py)-B3LYP-D3/6-31G**;LANL2DZ(Bi).

Neutral species. In view of the dinuclear structures $[BiX_3(py)_2]_2$ found in the solid state, DFT calculations were performed in order to obtain indications towards the minimum structure of these compounds (Figure S12). The successive addition of pyridine ligands to $BiCl_3$ according to $BiCl_3$ + n py → $[BiCl_3(py)_n]$ is exothermal and exergonic for the addition of up to four pyridine ligands (Table S9). Compounds featuring meridional coordination geometries are slightly lower in energies than isomers with a facial arrangement of the chloride ligands. Among the structures considered in this study, the formation of the dinuclear species $[BiX_3(py)_2]_2$ is most exothermal. It has to be kept in mind, however, that the solvation of two bismuth atoms contributes to the overall thermodynamic data. The formation of the dimer $[BiX_3(py)_2]_2$ from $[BiCl_3(py)_4]$ according to the reaction 2 $[BiCl_3(py)_4]$ → $[BiX_3(py)_2]_2$ + 4 py is somewhat exergonic when a concetration correction is not taken into account (ΔG = –8.1 kcal mol^{-1}) and somewhat endergonic when a concentration correction is performed as described above (ΔG = +3.6 kcal mol^{-1}). Thus, it is suggested that $[BiX_3(py)_2]_2$ is likely to be accessible in solution.

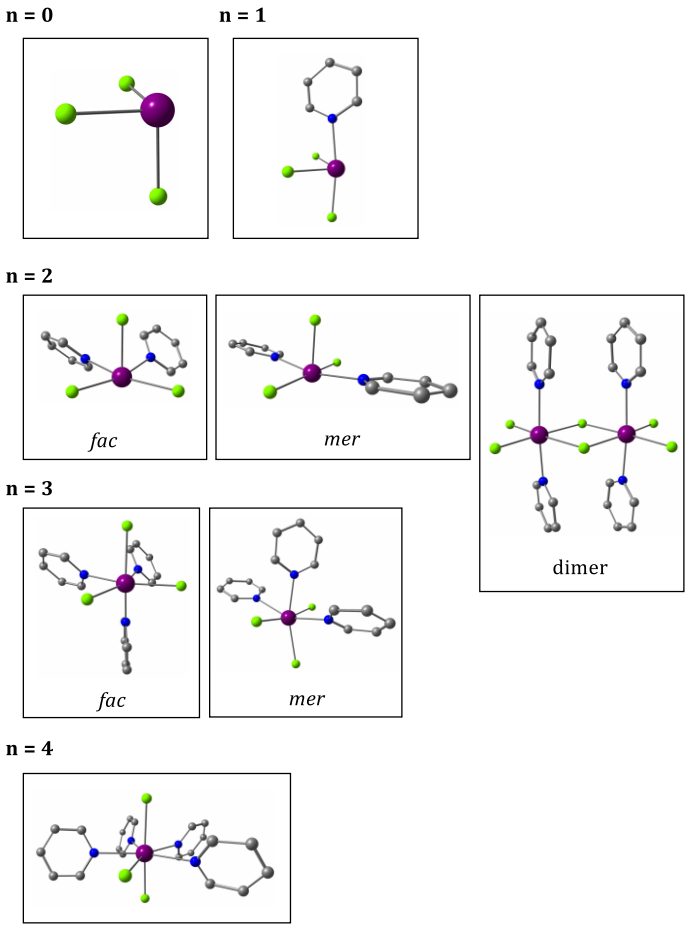

Figure S12. 3D structures of the $[BiCl_3(py)_n]$ systems computed herein. Level of theory: PCM(py)-B3LYP-D3/6-31G**;LANL2DZ(Bi).

Energies of Compounds Investigated by DFT Calculations

Table S9. Energies of the computed cationic systems. Gibbs free energies include concentration correction. Level of theory: PCM(py)-B3LYP-D3/6-31G**;LANL2DZ(Bi) level of theory.

Entry	Compound	*H* [hartree]	*G* [hartree]
1	Cl^-	-460.359429	-460.373795
2	py	-248.207281	-248.234504
3	$BiCl_3$	-1386.145606	-1386.182874
4	$[BiCl_3(py)]$	-1634.374759	-1634.428153
5	$[BiCl_3(py)_2]$ (A)	-1882.607026	-1882.676734
6	$[BiCl_3(py)_2]$ (B)	-1882.604293	-1882.673471
7	$[BiCl_3(py)_3]$ (A)	-2130.836337	-2130.917999
8	$[BiCl_3(py)_3]$ (B)	-2130.833733	-2130.913161
9	$[BiCl_3(py)_4]$	-2379.058805	-2379.157894
10	$[BiCl_3(py)_2]_2$	-3765.24825	-3765.372091
11	$[BiCl(py)_5]^{2+}$	-1706.488228	-1706.586012
13	$BiCl_2^+$	-925.685339	-925.718620
12	$[BiCl_2(py)]^+$	-1173.963536	-1174.010288
14	$[BiCl_2(py)_2]^+$ (A)	-1422.202156	-1422.263357
15	$[BiCl_2(py)_2]^+$ (B)	-1422.200650	-1422.262095
16	$[BiCl_2(py)_2]^+$ (C)	-1422.200388	-1422.259844
17	$[BiCl_2(py)_3]^+$ (A)	-1670.442747	-1670.517439
18	$[BiCl_2(py)_3]^+$ (B)	-1670.433860	-1670.512035
19	$[BiCl_2(py)_3]^+$ (C)	-1670.435805	-1670.510850
20	$[BiCl_2(py)_4]^+$ (A)	-1918.669885	-1918.761247
21	$[BiCl_2(py)_4]^+$ (B)	-1918.666331	-1918.759296
22	$[BiCl_2(py)_4]^+$ (C)	-1918.661375	-1918.753129
23	$[BiCl_2(py)_4]^+$ (D)	-1918.657629	-1918.747585
24	$[BiCl_2(py)_5]^+$ (A)	-2166.900358	-2167.011338
25	$[BiCl_2(py)_5]^+$ (B)	-2166.885155	-2166.992749
26	$[BiCl_2(py)_6]^+$	-2415.098015	-2415.227711
27	$[BiCl_2(py)_4]$[BArF]	-5566.236982	-5566.455596

NMR Spectra of Isolated Complexes

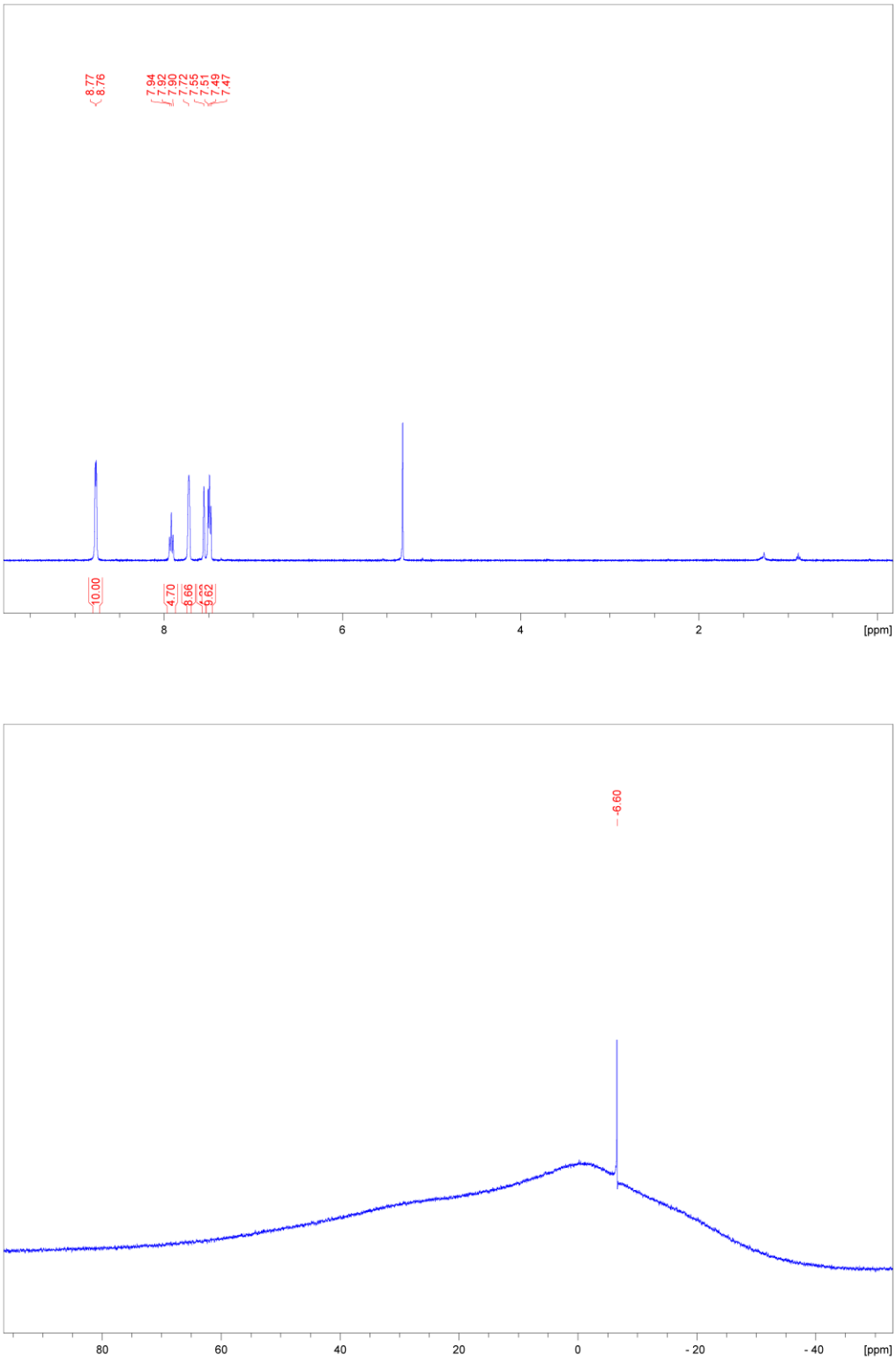

Figure S13. ^{1}H and ^{11}B NMR spectra of $[BiCl_2(py)_5][BArF]$ (**1-Cl**) in CD_2Cl_2.

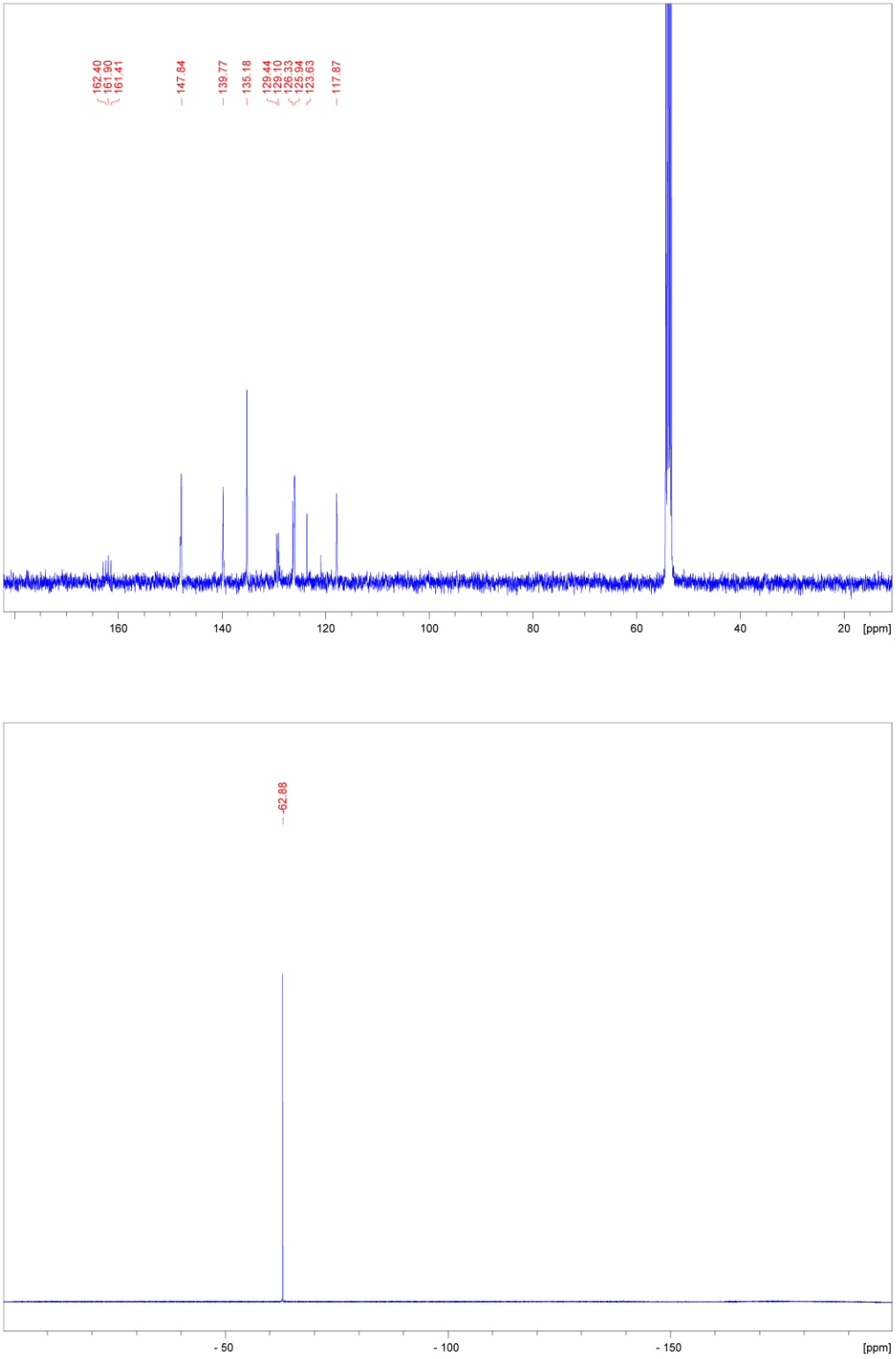

Figure S14. ^{13}C and ^{19}F NMR spectra $[BiCl_2(py)_5][BArF]$ (**1-Cl**) in CD_2Cl_2.

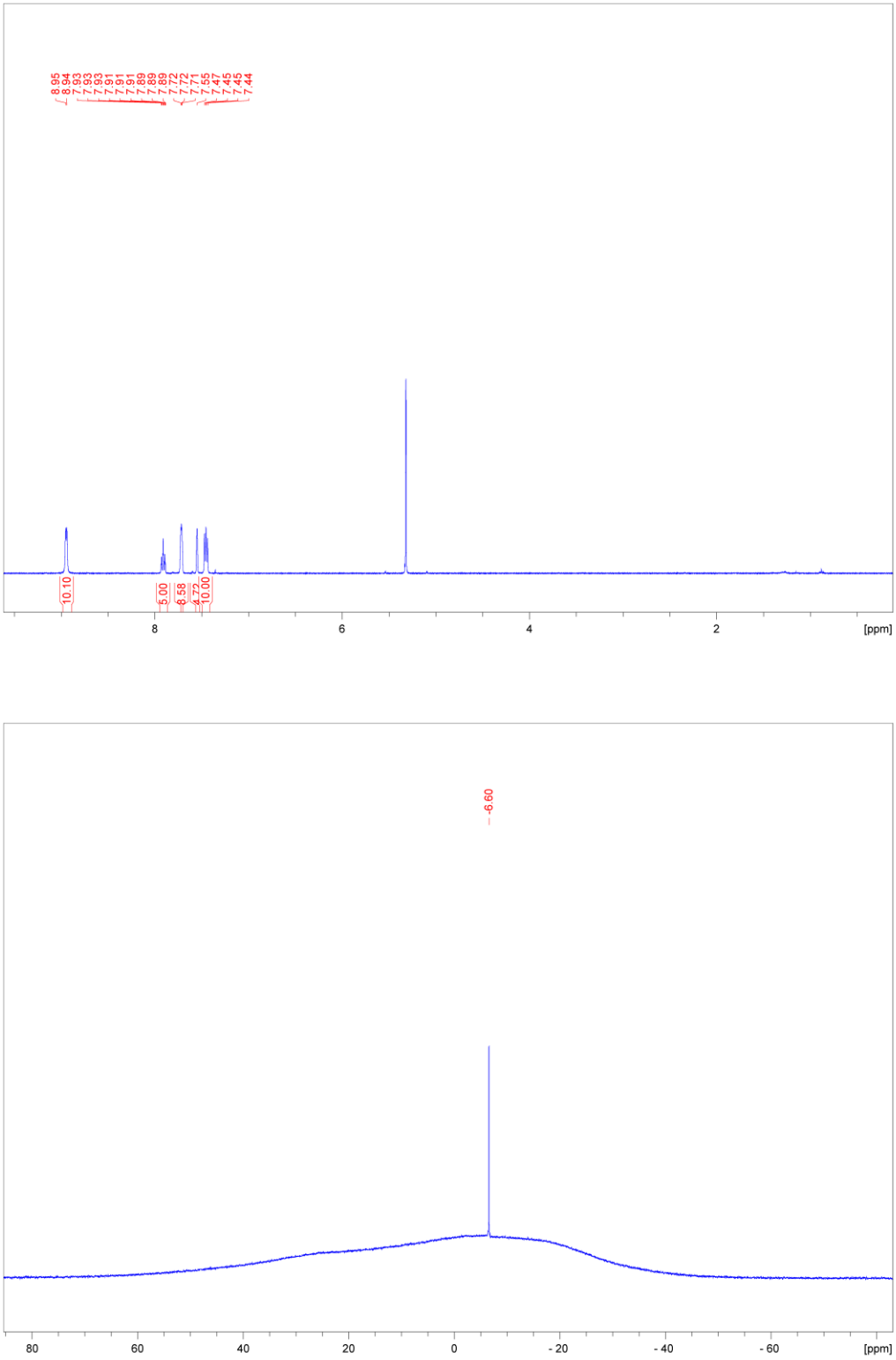

Figure S15. ^{1}H and ^{11}B NMR spectra of $[BiBr_2(py)_5][BArF]$ (**1-Br**) in CD_2Cl_2.

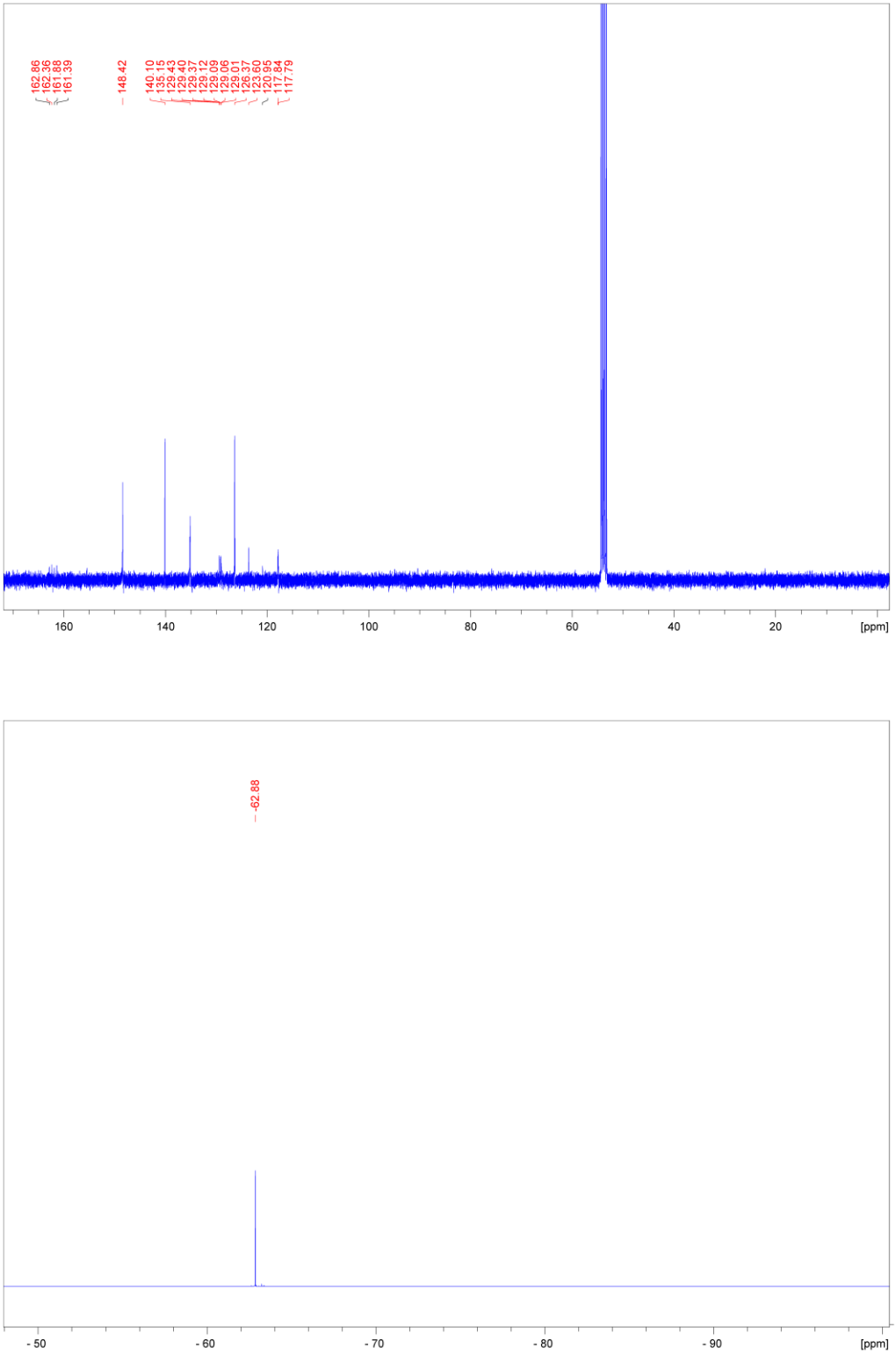

Figure S 16. ^{13}C and ^{19}F NMR spectra $[BiBr_2(py)_5][BArF]$ (**1-Br**) in CD_2Cl_2.

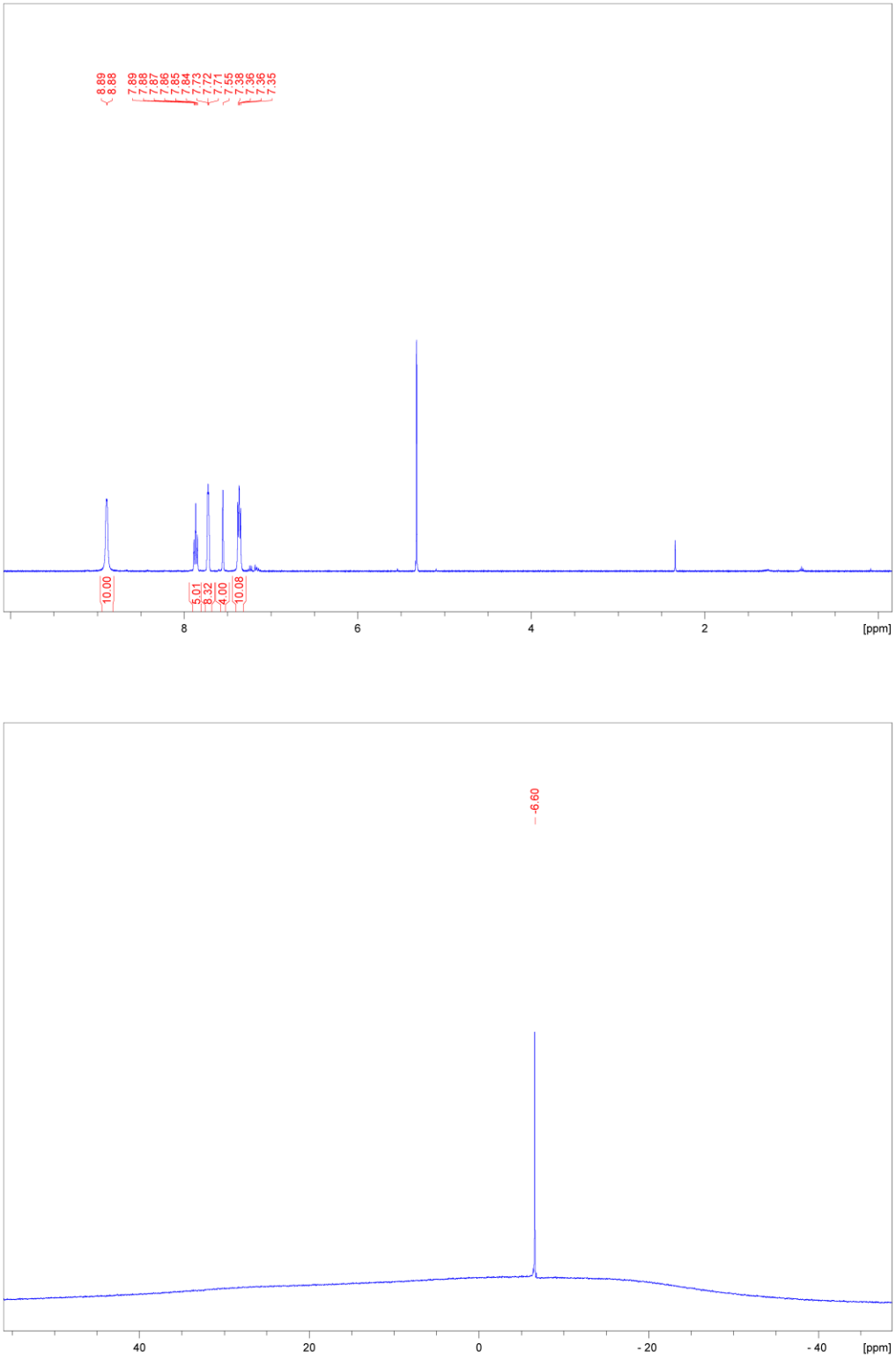

Figure S17. ^{1}H and ^{11}B NMR spectra of $[BiI_2(py)_5][BArF]$ (**1-I**) in CD_2Cl_2.

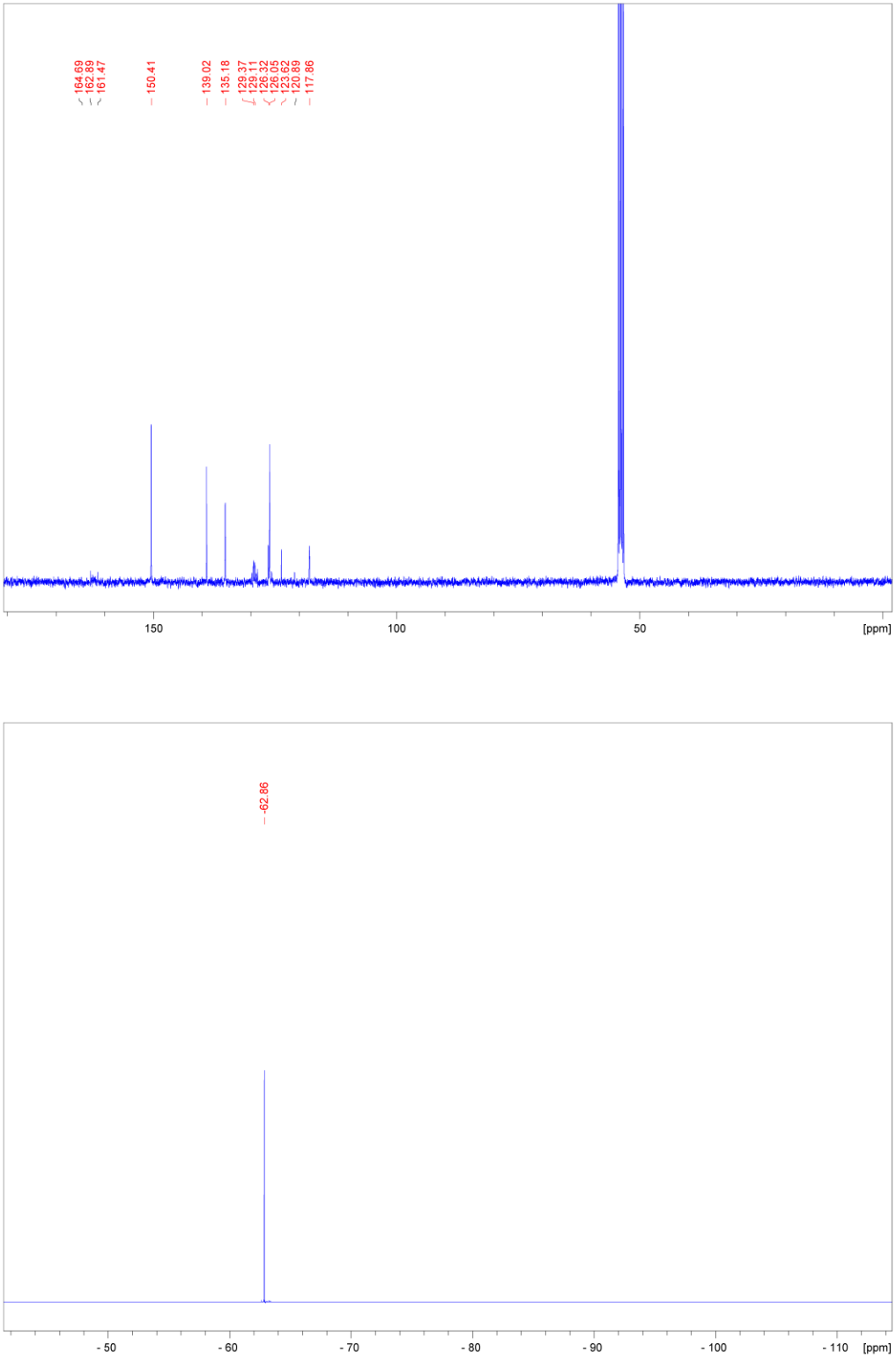

Figure S18. ^{13}C and ^{19}F NMR spectra $[BiI_2(py)_5][BArF]$ (**1-I**) in CD_2Cl_2.

Cartesian coordinates (Angstrom)

[$BiCl_3(py)$]

Bi	-0.717235000	-0.003771000	-0.388993000
Cl	-0.600054000	1.888932000	1.229045000
Cl	-0.580255000	-1.852978000	1.277769000
N	1.829946000	0.002384000	-0.133312000
C	2.512173000	-1.158088000	-0.140221000
H	1.922441000	-2.068897000	-0.142969000
C	3.902629000	-1.203697000	-0.126658000
H	4.409086000	-2.162125000	-0.129400000
C	4.614209000	-0.003821000	-0.105678000
H	5.699280000	-0.006256000	-0.092741000
C	3.907551000	1.199073000	-0.099317000
H	4.418131000	2.155120000	-0.079939000
C	2.516752000	1.159871000	-0.114531000
H	1.930305000	2.072580000	-0.097925000
Cl	-3.312527000	-0.015608000	-0.313812000

[$BiCl_3(py)_2$] (A)

Bi	-0.000035000	-0.000028000	-0.390084000
Cl	-0.000119000	2.686141000	-0.417250000
Cl	-0.000004000	-2.685945000	-0.417173000
N	-2.486917000	-0.001819000	-0.062132000
C	-3.172492000	1.157299000	-0.040825000
C	-3.151965000	-1.161808000	0.100364000
C	-4.550850000	1.196024000	0.142901000
H	-2.591464000	2.064822000	-0.168993000
C	-4.529479000	-1.202162000	0.289241000
H	-2.555263000	-2.067923000	0.078062000
C	-5.242975000	-0.003480000	0.310888000
H	-5.062993000	2.151390000	0.154577000
H	-5.024836000	-2.157865000	0.417255000
H	-6.318260000	-0.004072000	0.457286000
N	2.486914000	0.001762000	-0.062792000
C	3.151885000	1.161758000	0.099970000
C	3.172500000	-1.157336000	-0.041339000
C	4.529331000	1.202123000	0.289317000
H	2.555196000	2.067877000	0.077499000
C	4.550802000	-1.196053000	0.142837000
H	2.591527000	-2.064857000	-0.169758000
C	5.242842000	0.003447000	0.311150000
H	5.024623000	2.157834000	0.417550000
H	5.062952000	-2.151412000	0.154615000
H	6.318072000	0.004052000	0.457944000
Cl	0.000460000	0.000039000	2.113738000

$[BiCl_3(py)_2]$ (B)

Bi	0.025792000	-0.907643000	-0.298672000
Cl	-0.123661000	-0.736866000	2.199806000
C	-1.457806000	2.063102000	-1.038020000
H	-0.566873000	2.062572000	-1.659210000
N	-1.621102000	1.011854000	-0.214011000
Cl	-2.034676000	-2.553713000	-0.270213000
C	-2.371500000	3.110123000	-1.094717000
H	-2.199418000	3.940581000	-1.769771000
C	-2.707763000	0.960528000	0.577134000
H	-2.795070000	0.089993000	1.218333000
C	-3.668001000	1.967494000	0.578567000
H	-4.528504000	1.889317000	1.233161000
C	-3.496600000	3.061777000	-0.270126000
H	-4.227811000	3.863357000	-0.289645000
N	1.634509000	1.031688000	0.002183000
C	1.379122000	2.064919000	0.825575000
C	2.770425000	1.034861000	-0.719105000
C	2.246180000	3.145463000	0.948643000
H	0.460803000	2.008202000	1.399256000
C	3.688861000	2.078073000	-0.651708000
H	2.947964000	0.169950000	-1.350793000
C	3.420986000	3.153908000	0.195237000
H	2.001844000	3.957243000	1.624213000
H	4.592623000	2.039671000	-1.248992000
H	4.117611000	3.982565000	0.270452000
Cl	2.107681000	-2.522092000	-0.121555000

$[BiCl_3(py)_3]$ (A)

Bi	0.000011000	0.768762000	-0.000011000
N	2.473566000	0.242940000	-0.089965000
Cl	0.159579000	0.471988000	2.680686000
Cl	-0.159553000	0.471956000	-2.680711000
N	-0.000032000	-1.760427000	0.000009000
N	-2.473600000	0.243033000	0.089959000
C	3.262153000	0.442940000	0.982762000
H	2.778387000	0.837682000	1.870318000
C	4.620758000	0.142753000	0.966751000
H	5.220289000	0.318881000	1.852615000
C	5.179931000	-0.383687000	-0.198085000
H	6.236154000	-0.629425000	-0.239950000
C	4.359725000	-0.589603000	-1.308082000
H	4.751911000	-0.996719000	-2.233141000
C	3.010811000	-0.262003000	-1.216313000
H	2.333789000	-0.398716000	-2.053638000
C	0.743315000	-2.442528000	0.889834000
H	1.313669000	-1.850428000	1.596541000

C	0.772926000	-3.833142000	0.919936000
H	1.388908000	-4.341824000	1.652752000
C	-0.000105000	-4.542304000	0.000054000
H	-0.000134000	-5.627553000	0.000072000
C	-0.773097000	-3.833130000	-0.919852000
H	-1.389106000	-4.341804000	-1.652651000
C	-0.743413000	-2.442518000	-0.889794000
H	-1.313735000	-1.850410000	-1.596521000
C	-3.010881000	-0.261775000	1.216350000
H	-2.333878000	-0.398423000	2.053700000
C	-4.359807000	-0.589323000	1.308131000
H	-4.752022000	-0.996330000	2.233226000
C	-5.179988000	-0.383500000	0.198098000
H	-6.236219000	-0.629201000	0.239971000
C	-4.620778000	0.142801000	-0.966784000
H	-5.220288000	0.318854000	-1.852677000
C	-3.262163000	0.442945000	-0.982801000
H	-2.778370000	0.837580000	-1.870391000
Cl	0.000202000	3.480421000	-0.000006000

$[BiCl_3(py)_3]$ (B)

Cl	-0.231273000	-0.546047000	2.645677000
Bi	-0.074206000	-0.793656000	-0.033271000
Cl	-1.242799000	-3.246575000	-0.073909000
C	-2.745119000	0.917485000	-1.055297000
H	-1.992790000	1.209226000	-1.779772000
N	-2.355092000	0.050452000	-0.102012000
C	-4.045795000	1.404242000	-1.114061000
H	-4.322270000	2.101823000	-1.896182000
C	-3.241646000	-0.369409000	0.820255000
H	-2.872392000	-1.067039000	1.563230000
C	-4.559191000	0.074574000	0.823716000
H	-5.243721000	-0.284552000	1.583397000
C	-4.968709000	0.977327000	-0.158249000
H	-5.990820000	1.341123000	-0.179324000
N	0.239165000	1.703282000	0.042548000
C	1.065487000	2.309335000	-0.829750000
C	-0.381385000	2.445268000	0.978251000
C	1.303172000	3.679548000	-0.795674000
H	1.529978000	1.674856000	-1.575383000
C	-0.200440000	3.821161000	1.072860000
H	-1.025760000	1.911783000	1.667554000
C	0.658496000	4.450822000	0.171640000
H	1.978551000	4.125060000	-1.517115000
H	-0.723515000	4.379597000	1.840742000
H	0.821929000	5.522479000	0.221960000

N	0.047401000	-0.478586200	-2.227432060
C	0.327183800	-1.493736530	-3.067761480
C	-0.155524880	0.735944500	-2.774447570
C	0.414936470	-1.343896050	-4.463882180
H	0.488972810	-2.478034560	-2.593328750
C	-0.089202930	0.985546930	-4.157503880
H	-0.382971060	1.549944150	-2.063151000
C	0.201915700	-0.078256100	-5.013263010
H	0.646341890	-2.206979630	-5.100975140
H	-0.263549450	1.996329700	-4.547744350
H	0.261252660	0.077293970	-6.099847220
Cl	2.544123000	-0.514445000	0.073406000

$[BiCl_3(py)_4]$

Bi	-0.000130000	-0.583533000	-0.000197000
N	1.490290000	1.629371000	-0.048518000
Cl	0.099501000	-0.359964000	2.701633000
Cl	-0.099211000	-0.359453000	-2.701928000
N	2.506596000	-1.148743000	-0.049115000
N	-2.507053000	-1.148596000	0.048414000
N	-1.490479000	1.629534000	0.049779000
C	2.249024000	1.961570000	1.008708000
H	2.220978000	1.278213000	1.851846000
C	3.023517000	3.118866000	1.040101000
H	3.619067000	3.346778000	1.917267000
C	3.011802000	3.963722000	-0.070325000
H	3.604464000	4.873095000	-0.078736000
C	2.224458000	3.618732000	-1.169413000
H	2.184737000	4.244471000	-2.054240000
C	1.478004000	2.443799000	-1.116413000
H	0.852865000	2.132220000	-1.947525000
C	3.123983000	-1.621266000	1.046232000
H	2.500914000	-1.768751000	1.923109000
C	4.488245000	-1.899350000	1.067095000
H	4.948301000	-2.275730000	1.973942000
C	5.234824000	-1.684255000	-0.091892000
H	6.300013000	-1.892051000	-0.108199000
C	4.589727000	-1.198163000	-1.229943000
H	5.130392000	-1.018475000	-2.152500000
C	3.223272000	-0.940302000	-1.166021000
H	2.676312000	-0.559384000	-2.023645000
C	-3.223372000	-0.941413000	1.165769000
H	-2.676088000	-0.561725000	2.023738000
C	-4.589883000	-1.199019000	1.229739000
H	-5.130240000	-1.020380000	2.152681000
C	-5.235411000	-1.683481000	0.091245000

H	-6.300647000	-1.891033000	0.107564000
C	-4.489197000	-1.897259000	-1.068228000
H	-4.949604000	-2.272344000	-1.975434000
C	-3.124865000	-1.619532000	-1.047377000
H	-2.502081000	-1.766023000	-1.924627000
C	-2.247730000	1.962842000	-1.008180000
H	-2.219420000	1.279711000	-1.851502000
C	-3.021114000	3.120860000	-1.039988000
H	-3.615454000	3.349704000	-1.917732000
C	-3.009873000	3.965244000	0.070816000
H	-3.601672000	4.875182000	0.078911000
C	-2.224177000	3.619027000	1.170695000
H	-2.184956000	4.244325000	2.055856000
C	-1.478720000	2.443430000	1.118060000
H	-0.854898000	2.130806000	1.949788000
Cl	-0.000453000	-3.294147000	0.000753000

$[BiCl_3(py)_2]_2$

Bi	-0.000267000	2.145636000	-0.090820000
C	-3.164177000	1.458352000	-1.112914000
H	-2.546374000	1.063910000	-1.912901000
N	-2.519072000	2.038453000	-0.082467000
Cl	-0.000411000	0.062197000	1.972171000
Cl	-0.000420000	3.823387000	-2.048221000
C	-4.550349000	1.356490000	-1.150977000
H	-5.030321000	0.879114000	-1.997173000
C	-3.231483000	2.528240000	0.948771000
H	-2.665142000	2.988553000	1.752192000
C	-4.620752000	2.458145000	0.985023000
H	-5.157353000	2.863147000	1.835348000
C	-5.292190000	1.865305000	-0.084387000
H	-6.375086000	1.795813000	-0.084245000
C	3.230968000	2.528934000	0.948548000
H	2.664548000	2.989330000	1.751873000
N	2.518601000	2.038972000	-0.082622000
Cl	0.000141000	-0.063012000	-1.971443000
Cl	-0.000256000	3.954659000	1.766189000
C	4.620243000	2.459016000	0.984819000
H	5.156801000	2.864205000	1.835084000
C	3.163747000	1.458934000	-1.113076000
H	2.545979000	1.064425000	-1.913044000
C	4.549930000	1.357090000	-1.151049000
H	5.029958000	0.879726000	-1.997213000
C	5.291720000	1.866040000	-0.084475000
H	6.374624000	1.796728000	-0.084350000
Bi	0.000138000	-2.146424000	0.091483000

C	3.164045000	-1.457104000	1.112284000
H	2.546293000	-1.062749000	1.912340000
N	2.518914000	-2.037917000	0.082255000
Cl	0.001961000	-3.824673000	2.048545000
C	4.550156000	-1.354052000	1.149634000
H	5.030145000	-0.875889000	1.995374000
C	3.231250000	-2.527545000	-0.949112000
H	2.664911000	-2.988519000	-1.752155000
C	4.620461000	-2.456591000	-0.985907000
H	5.157009000	-2.861526000	-1.836298000
C	5.291911000	-1.862775000	0.082944000
H	6.374753000	-1.792473000	0.082299000
C	-3.230885000	-2.528735000	-0.948851000
H	-2.664305000	-2.989765000	-1.751698000
N	-2.518813000	-2.038908000	0.082604000
Cl	0.000561000	-3.954782000	-1.766282000
C	-4.620101000	-2.458042000	-0.985919000
H	-5.156424000	-2.863266000	-1.836313000
C	-3.164218000	-1.458048000	1.112426000
H	-2.546676000	-1.063591000	1.912598000
C	-4.550359000	-1.355374000	1.149588000
H	-5.030580000	-0.877341000	1.995271000
C	-5.291844000	-1.864367000	0.082831000
H	-6.374706000	-1.794372000	0.082049000

$[BiCl(py)_5]^{2+}$

Bi	0.000922000	0.001129000	-0.147226000
N	0.670625000	-2.482401000	-0.146055000
Cl	-0.005704000	0.002543000	2.547435000
N	-2.155001000	-1.403741000	-0.148990000
N	0.919672000	2.403616000	-0.142301000
N	-2.002634000	1.614000000	-0.151362000
N	2.570485000	-0.131593000	-0.147686000
C	1.225861000	-3.038025000	0.945086000
H	1.360185000	-2.385892000	1.802967000
C	1.601001000	-4.377728000	0.986241000
H	2.043892000	-4.786117000	1.887634000
C	1.394398000	-5.167917000	-0.145306000
H	1.676765000	-6.215712000	-0.145075000
C	0.818059000	-4.589435000	-1.276914000
H	0.638208000	-5.165926000	-2.177360000
C	0.468954000	-3.242750000	-1.236293000
H	0.019844000	-2.748035000	-2.092483000
C	-2.504724000	-2.119778000	0.934069000
H	-1.836443000	-2.060843000	1.787764000
C	-3.663553000	-2.889892000	0.971937000

H	-3.909331000	-3.450504000	1.866764000
C	-4.486371000	-2.920765000	-0.154701000
H	-5.396359000	-3.511985000	-0.156787000
C	-4.121537000	-2.177857000	-1.278151000
H	-4.730721000	-2.172965000	-2.174974000
C	-2.947781000	-1.431283000	-1.234528000
H	-2.620758000	-0.840421000	-2.084882000
C	-2.803069000	1.709079000	0.924391000
H	-2.546919000	1.080351000	1.771727000
C	-3.896611000	2.569176000	0.962786000
H	-4.514952000	2.615928000	1.852090000
C	-4.170518000	3.356560000	-0.156429000
H	-5.016439000	4.036411000	-0.158650000
C	-3.339964000	3.255217000	-1.273283000
H	-3.517310000	3.846084000	-2.164818000
C	-2.264907000	2.372253000	-1.230086000
H	-1.595261000	2.254373000	-2.076517000
C	0.764239000	3.191132000	0.936275000
H	0.243861000	2.753029000	1.782552000
C	1.246652000	4.495953000	0.978432000
H	1.100024000	5.096847000	1.868871000
C	1.913459000	5.001599000	-0.138216000
H	2.300498000	6.015592000	-0.136480000
C	2.073777000	4.183166000	-1.257061000
H	2.584633000	4.535118000	-2.146145000
C	1.562696000	2.889154000	-1.218566000
H	1.658260000	2.217794000	-2.066460000
C	3.229569000	-0.569534000	-1.234555000
H	2.619070000	-0.848534000	-2.088194000
C	4.618033000	-0.655896000	-1.276221000
H	5.109436000	-1.013304000	-2.174136000
C	5.348385000	-0.276384000	-0.149334000
H	6.432234000	-0.332544000	-0.150147000
C	4.662828000	0.177799000	0.978109000
H	5.189852000	0.483491000	1.874875000
C	3.272781000	0.236364000	0.938084000
H	2.696237000	0.580400000	1.791424000

$[BiCl_2(py)]^+$

Bi	-0.908632000	-0.016462000	-0.475462000
Cl	-1.185589000	1.870557000	1.064751000
Cl	-1.148927000	-1.815636000	1.173970000
N	1.353124000	0.004676000	-0.106356000
C	2.032383000	-1.165339000	-0.075049000
H	1.453620000	-2.078580000	-0.141790000
C	3.412196000	-1.190282000	0.058772000

H	3.924755000	-2.144251000	0.082736000
C	4.105903000	0.016306000	0.164313000
H	5.185292000	0.020867000	0.269272000
C	3.394092000	1.216420000	0.137992000
H	3.892139000	2.174355000	0.225575000
C	2.014581000	1.179877000	0.001081000
H	1.420587000	2.085638000	-0.008837000

$[BiCl_2(py)_2]^+$ (A)

Bi	0.000116000	-0.000223000	-0.451171000
Cl	-0.000610000	1.890493000	1.145299000
Cl	0.000031000	-1.889615000	1.146665000
N	2.440258000	0.000085000	-0.096058000
C	3.122396000	1.162789000	-0.059056000
C	3.122512000	-1.162625000	-0.059635000
C	4.509591000	1.201835000	0.018522000
H	2.537141000	2.075425000	-0.078180000
C	4.509679000	-1.201580000	0.017930000
H	2.537368000	-2.075318000	-0.079293000
C	5.217113000	0.000155000	0.058076000
H	5.016560000	2.159118000	0.050454000
H	5.016760000	-2.158819000	0.049413000
H	6.300208000	0.000163000	0.120715000
N	-2.440285000	0.000544000	-0.096627000
C	-3.122878000	1.162931000	-0.059571000
C	-3.122037000	-1.162462000	-0.059903000
C	-4.510074000	1.201425000	0.018358000
H	-2.537958000	2.075781000	-0.078985000
C	-4.509166000	-1.201995000	0.018073000
H	-2.536533000	-2.074926000	-0.079592000
C	-5.217086000	-0.000537000	0.058314000
H	-5.017426000	2.158507000	0.050283000
H	-5.015850000	-2.159435000	0.049826000
H	-6.300162000	-0.000950000	0.121272000

$[BiCl_2(py)_2]^+$ (B)

Bi	0.619360000	-0.887486000	-0.366512000
Cl	0.462659000	-1.422955000	2.036874000
Cl	3.172182000	-0.574380000	-0.332268000
N	-1.849667000	-0.405996000	-0.229776000
C	-2.682272000	-1.002305000	0.645380000
C	-2.365807000	0.399937000	-1.179226000
C	-4.058880000	-0.804791000	0.605416000
H	-2.224831000	-1.638271000	1.395050000
C	-3.728994000	0.646600000	-1.283424000
H	-1.662331000	0.861385000	-1.865687000
C	-4.592163000	0.033996000	-0.373254000

H	-4.692679000	-1.299964000	1.331814000
H	-4.099125000	1.305558000	-2.060144000
H	-5.661702000	0.208003000	-0.426579000
N	0.570033000	1.374697000	0.085115000
C	-0.185517000	1.858046000	1.095677000
C	1.301595000	2.218519000	-0.676750000
C	-0.237072000	3.216322000	1.371027000
H	-0.740395000	1.138871000	1.684404000
C	1.282715000	3.588304000	-0.457492000
H	1.913673000	1.779366000	-1.455032000
C	0.503121000	4.097566000	0.581453000
H	-0.847896000	3.567649000	2.193765000
H	1.876974000	4.235082000	-1.091517000
H	0.476236000	5.164251000	0.775862000

$[BiCl_2(py)_2]^+$ (C)

Bi	-0.000192000	-1.175972000	0.000100000
Cl	0.402196000	-0.931294000	-2.581376000
Cl	-0.402566000	-0.930599000	2.581442000
N	1.543771000	0.523869000	0.202782000
N	-1.543733000	0.524094000	-0.202883000
C	2.647993000	0.522413000	-0.579622000
H	2.736731000	-0.272240000	-1.309618000
C	3.611395000	1.514199000	-0.466886000
H	4.484883000	1.478650000	-1.106653000
C	3.428148000	2.537101000	0.463795000
H	4.164904000	3.326670000	0.564953000
C	2.284120000	2.530832000	1.263078000
H	2.100008000	3.306294000	1.996761000
C	1.362333000	1.505440000	1.115882000
H	0.472826000	1.448891000	1.730417000
C	-1.361446000	1.505882000	-1.115609000
H	-0.471758000	1.449048000	-1.729840000
C	-2.282703000	2.531735000	-1.262854000
H	-2.098017000	3.307374000	-1.996200000
C	-3.427103000	2.538204000	-0.464096000
H	-4.163477000	3.328151000	-0.565288000
C	-3.611267000	1.515028000	0.466125000
H	-4.485153000	1.479556000	1.105361000
C	-2.648340000	0.522801000	0.578975000
H	-2.737740000	-0.272066000	1.308654000

$[BiCl_2(py)_3]^+$ (A)

Bi	0.000003000	-0.955631000	-0.000134000
N	-2.401069000	-0.416558000	-0.075560000
Cl	-0.119390000	-0.684985000	2.632107000
Cl	0.119436000	-0.683958000	-2.632243000

N	0.000071000	1.383567000	0.000312000
N	2.401152000	-0.416588000	0.075385000
C	-3.206314000	-0.808091000	0.932642000
H	-2.728677000	-1.293987000	1.776700000
C	-4.577762000	-0.581656000	0.907164000
H	-5.190236000	-0.910230000	1.738673000
C	-5.132603000	0.071838000	-0.193541000
H	-6.199331000	0.264606000	-0.238906000
C	-4.295138000	0.474917000	-1.234722000
H	-4.683720000	0.985934000	-2.107914000
C	-2.933796000	0.211607000	-1.142817000
H	-2.245546000	0.498636000	-1.930475000
C	-0.764691000	2.062748000	0.882071000
H	-1.348262000	1.476477000	1.579172000
C	-0.789575000	3.450101000	0.906230000
H	-1.419129000	3.956037000	1.628325000
C	-0.000262000	4.158914000	0.000531000
H	-0.000395000	5.243653000	0.000600000
C	0.789236000	3.450426000	-0.905270000
H	1.418675000	3.956634000	-1.627273000
C	0.764679000	2.063072000	-0.881339000
H	1.348415000	1.477041000	-1.578501000
C	2.933878000	0.211081000	1.142935000
H	2.245630000	0.497674000	1.930756000
C	4.295204000	0.474433000	1.234924000
H	4.683786000	0.985036000	2.108360000
C	5.132654000	0.071947000	0.193502000
H	6.199362000	0.264794000	0.238909000
C	4.577817000	-0.581040000	-0.907503000
H	5.190273000	-0.909125000	-1.739216000
C	3.206383000	-0.807565000	-0.933037000
H	2.728756000	-1.293082000	-1.777320000

$[BiCl_2(py)_3]^+$ (B)

Bi	-0.009752000	-0.651225000	-0.369370000
N	-2.416147000	-0.274027000	-0.154214000
C	-3.169934000	-1.081062000	0.617162000
C	-3.006275000	0.710012000	-0.860650000
C	-4.547842000	-0.924978000	0.712332000
H	-2.645938000	-1.860123000	1.159966000
C	-4.378004000	0.927726000	-0.813611000
H	-2.359769000	1.335671000	-1.467323000
C	-5.162690000	0.096500000	-0.012837000
H	-5.120474000	-1.593881000	1.344051000
H	-4.814295000	1.732758000	-1.393236000
H	-6.236251000	0.242358000	0.044408000

N	2.452063000	-0.477362000	0.010201000
C	2.985995000	0.336527000	0.941049000
C	3.271147000	-1.165095000	-0.808863000
C	4.360177000	0.493893000	1.081605000
H	2.288073000	0.860254000	1.584312000
C	4.655570000	-1.064765000	-0.726154000
H	2.801947000	-1.812592000	-1.543851000
C	5.210293000	-0.218909000	0.234935000
H	4.748895000	1.160793000	1.842435000
H	5.277998000	-1.639563000	-1.402001000
H	6.286940000	-0.117975000	0.323473000
Cl	-0.358550000	-3.234876000	-0.202819000
N	0.093375000	1.853405000	-0.128976000
C	-0.618740000	2.543714000	0.782318000
C	0.870705000	2.525801000	-0.999760000
C	-0.579560000	3.931954000	0.852050000
H	-1.220373000	1.958480000	1.468612000
C	0.966975000	3.912808000	-0.990282000
H	1.432191000	1.932868000	-1.715850000
C	0.227306000	4.629122000	-0.048237000
H	-1.169378000	4.448766000	1.600195000
H	1.608525000	4.413316000	-1.706176000
H	0.279720000	5.712332000	-0.015656000
Cl	-0.098164000	-0.550736000	2.125108000

$[BiCl_2(py)_3]^+$ (C)

Bi	-0.016084000	-0.481777000	-1.036896000
N	0.046304000	-0.817619000	1.267467000
C	0.094560000	-2.076569000	1.752005000
C	0.037397000	0.230404000	2.120902000
C	0.137454000	-2.326208000	3.117183000
H	0.098498000	-2.879685000	1.026404000
C	0.078094000	0.048196000	3.495051000
H	-0.003437000	1.220261000	1.685383000
C	0.129778000	-1.250468000	4.004458000
H	0.176298000	-3.350595000	3.467531000
H	0.069423000	0.914140000	4.145954000
H	0.163224000	-1.420217000	5.075239000
N	-1.880852000	1.041438000	-0.209681000
C	-1.994201000	2.282569000	-0.718106000
C	-2.824555000	0.600181000	0.644608000
C	-3.038744000	3.135682000	-0.377958000
H	-1.230851000	2.598617000	-1.422147000
C	-3.899601000	1.390888000	1.033925000
H	-2.710162000	-0.413842000	1.010754000
C	-4.007583000	2.683131000	0.517982000

H	-3.085807000	4.128496000	-0.810018000
H	-4.633741000	0.994987000	1.726062000
H	-4.834578000	3.323995000	0.805326000
Cl	-1.841148000	-2.310447000	-0.982991000
N	1.829810000	1.109337000	-0.260721000
C	2.845286000	0.665528000	0.505705000
C	1.853756000	2.383807000	-0.693309000
C	3.908013000	1.482318000	0.874933000
H	2.799258000	-0.371999000	0.817232000
C	2.879390000	3.264608000	-0.366386000
H	1.030922000	2.707117000	-1.322545000
C	3.925398000	2.806445000	0.434759000
H	4.702465000	1.081627000	1.493837000
H	2.852618000	4.282994000	-0.736243000
H	4.740885000	3.467872000	0.708050000
Cl	1.869765000	-2.251404000	-1.091268000

$[BiCl_2(py)_4]^+$ (A)

Bi	0.000070000	0.444220000	-0.000332000
N	1.498540000	-1.470052000	-0.044331000
Cl	-0.099834000	0.283769000	-2.667968000
Cl	0.100056000	0.284948000	2.667305000
N	2.400264000	1.470435000	-0.029228000
N	-1.499029000	-1.469738000	0.045137000
N	-2.400071000	1.470821000	0.028805000
C	1.422623000	-2.371240000	-1.043034000
H	0.665693000	-2.196184000	-1.798879000
C	2.278315000	-3.464089000	-1.111638000
H	2.184029000	-4.166354000	-1.931664000
C	3.243308000	-3.629144000	-0.117679000
H	3.924780000	-4.472927000	-0.146314000
C	3.318052000	-2.692806000	0.914043000
H	4.050748000	-2.781775000	1.707606000
C	2.428401000	-1.625363000	0.918684000
H	2.441571000	-0.881932000	1.706878000
C	3.120404000	1.446711000	-1.165519000
H	2.640191000	0.999857000	-2.031479000
C	4.410183000	1.964412000	-1.238215000
H	4.956474000	1.922954000	-2.173785000
C	4.972755000	2.528169000	-0.091967000
H	5.976981000	2.938881000	-0.116113000
C	4.224519000	2.555217000	1.085616000
H	4.623003000	2.982943000	1.998675000
C	2.941096000	2.015865000	1.075409000
H	2.324816000	2.003895000	1.969966000
C	-2.942325000	2.012763000	-1.076890000

H	-2.327030000	1.998006000	-1.972074000
C	-4.225811000	2.551903000	-1.087201000
H	-4.625489000	2.976754000	-2.001079000
C	-4.972592000	2.528410000	0.091400000
H	-5.976850000	2.939051000	0.115495000
C	-4.408546000	1.968339000	1.238716000
H	-4.953716000	1.929728000	2.175062000
C	-3.118772000	1.450588000	1.166047000
H	-2.637300000	1.006469000	2.032715000
C	-2.427999000	-1.626417000	-0.918490000
H	-2.440471000	-0.884062000	-1.707726000
C	-3.317593000	-2.693924000	-0.913264000
H	-4.049529000	-2.783986000	-1.707406000
C	-3.243711000	-3.628892000	0.119745000
H	-3.925135000	-4.472695000	0.148892000
C	-2.279571000	-3.462478000	1.114317000
H	-2.185948000	-4.163697000	1.935317000
C	-1.423868000	-2.369684000	1.045054000
H	-0.667512000	-2.193702000	1.801278000

$[BiCl_2(py)_4]^+$ (B)

Bi	0.000000000	0.000000000	0.000000000
N	0.000000000	2.526561000	0.000000000
Cl	0.000000000	0.000000000	2.690547000
Cl	0.000000000	0.000000000	-2.690547000
N	2.526561000	0.000000000	0.000000000
N	-2.526561000	0.000000000	0.000000000
N	0.000000000	-2.526561000	0.000000000
C	0.239114000	3.207743000	1.137099000
H	0.418478000	2.614230000	2.027896000
C	0.248980000	4.598194000	1.176010000
H	0.447309000	5.107690000	2.112076000
C	0.000000000	5.306739000	0.000000000
H	0.000000000	6.391897000	0.000000000
C	-0.248980000	4.598194000	-1.176010000
H	-0.447309000	5.107690000	-2.112076000
C	-0.239114000	3.207743000	-1.137099000
H	-0.418478000	2.614230000	-2.027896000
C	3.207743000	-0.239114000	1.137099000
H	2.614230000	-0.418478000	2.027896000
C	4.598194000	-0.248980000	1.176010000
H	5.107690000	-0.447309000	2.112076000
C	5.306739000	0.000000000	0.000000000
H	6.391897000	0.000000000	0.000000000
C	4.598194000	0.248980000	-1.176010000
H	5.107690000	0.447309000	-2.112076000

C	3.207743000	0.239114000	-1.137099000
H	2.614230000	0.418478000	-2.027896000
C	-0.239114000	-3.207743000	1.137099000
H	-0.418478000	-2.614230000	2.027896000
C	-0.248980000	-4.598194000	1.176010000
H	-0.447309000	-5.107690000	2.112076000
C	0.000000000	-5.306739000	0.000000000
H	0.000000000	-6.391897000	0.000000000
C	0.248980000	-4.598194000	-1.176010000
H	0.447309000	-5.107690000	-2.112076000
C	0.239114000	-3.207743000	-1.137099000
H	0.418478000	-2.614230000	-2.027896000
C	-3.207743000	0.239114000	1.137099000
H	-2.614230000	0.418478000	2.027896000
C	-4.598194000	0.248980000	1.176010000
H	-5.107690000	0.447309000	2.112076000
C	-5.306739000	0.000000000	0.000000000
H	-6.391897000	0.000000000	0.000000000
C	-4.598194000	-0.248980000	-1.176010000
H	-5.107690000	-0.447309000	-2.112076000
C	-3.207743000	-0.239114000	-1.137099000
H	-2.614230000	-0.418478000	-2.027896000

$[BiCl_2(py)_4]^+$ (C)

Bi	-0.015461000	-0.140699000	-0.816733000
N	2.390766000	-0.399905000	-0.423029000
Cl	-0.075963000	-2.654671000	-1.581723000
Cl	0.726929000	1.265160000	-2.984223000
N	-0.011153000	2.073573000	0.565606000
N	0.049951000	-1.102503000	1.507648000
N	-2.621048000	-0.218132000	-0.522147000
C	2.885377000	-1.591296000	-0.031686000
H	2.171537000	-2.399185000	0.082321000
C	4.241295000	-1.781218000	0.205339000
H	4.599006000	-2.755873000	0.516128000
C	5.113419000	-0.705405000	0.033885000
H	6.176651000	-0.824211000	0.214172000
C	4.598544000	0.523980000	-0.378670000
H	5.239552000	1.384355000	-0.531430000
C	3.231514000	0.637229000	-0.603100000
H	2.793587000	1.566736000	-0.947123000
C	0.507400000	3.185531000	0.008963000
H	0.910392000	3.082028000	-0.993754000
C	0.511763000	4.414374000	0.662607000
H	0.944825000	5.279868000	0.174331000
C	-0.051466000	4.502539000	1.935307000

H	-0.064393000	5.446827000	2.469607000
C	-0.605851000	3.356287000	2.506780000
H	-1.063604000	3.377892000	3.489100000
C	-0.565557000	2.164414000	1.791494000
H	-0.991679000	1.257221000	2.204335000
C	-3.316038000	-1.334063000	-0.813771000
H	-2.737177000	-2.186589000	-1.156575000
C	-4.701028000	-1.402321000	-0.692196000
H	-5.217631000	-2.323753000	-0.935784000
C	-5.394840000	-0.272163000	-0.258894000
H	-6.474658000	-0.293941000	-0.153925000
C	-4.677259000	0.888483000	0.033009000
H	-5.174220000	1.792096000	0.367334000
C	-3.293622000	0.874003000	-0.112854000
H	-2.703475000	1.758614000	0.100720000
C	-0.809242000	-2.086791000	1.832604000
H	-1.482541000	-2.423097000	1.052754000
C	-0.831224000	-2.663315000	3.098244000
H	-1.541026000	-3.452957000	3.315584000
C	0.071080000	-2.209459000	4.060275000
H	0.079533000	-2.641498000	5.055456000
C	0.964749000	-1.191997000	3.721953000
H	1.685063000	-0.809718000	4.435837000
C	0.922671000	-0.664665000	2.437049000
H	1.597375000	0.128756000	2.136257000

$[BiCl_2(py)_4]^+$ (D)

Bi	0.022848000	-0.560416000	-0.308356000
N	-1.544307000	1.576293000	-0.054914000
Cl	0.097219000	-0.468649000	2.180128000
N	-2.404397000	-1.240105000	0.003841000
N	2.487745000	-1.099783000	-0.092194000
N	1.426232000	1.680553000	-0.154696000
C	-2.460929000	1.810389000	-1.009616000
H	-2.544336000	1.066542000	-1.796718000
C	-3.282656000	2.933817000	-1.003960000
H	-4.005076000	3.079661000	-1.799076000
C	-3.155184000	3.849229000	0.041379000
H	-3.782049000	4.734270000	0.078916000
C	-2.209803000	3.605447000	1.038189000
H	-2.078581000	4.287189000	1.870935000
C	-1.423167000	2.460095000	0.950114000
H	-0.672964000	2.233544000	1.700164000
C	-2.984409000	-1.952486000	-0.979005000
H	-2.342109000	-2.267445000	-1.794643000
C	-4.333557000	-2.291809000	-0.956477000

H	-4.758752000	-2.862319000	-1.774205000
C	-5.108043000	-1.890236000	0.132131000
H	-6.162261000	-2.142550000	0.182124000
C	-4.503438000	-1.160959000	1.156370000
H	-5.064566000	-0.831454000	2.023370000
C	-3.151236000	-0.851300000	1.052118000
H	-2.644264000	-0.278314000	1.819825000
C	3.340690000	-0.640445000	-1.025319000
H	2.925871000	0.006069000	-1.791979000
C	4.694917000	-0.957202000	-1.017427000
H	5.343985000	-0.566143000	-1.792476000
C	5.186077000	-1.772797000	0.002595000
H	6.238725000	-2.033401000	0.041482000
C	4.301157000	-2.248531000	0.970396000
H	4.637952000	-2.885444000	1.780289000
C	2.958059000	-1.895627000	0.884175000
H	2.232585000	-2.252518000	1.605913000
C	2.283820000	1.943576000	0.845990000
H	2.374662000	1.181590000	1.612815000
C	3.018003000	3.124781000	0.909713000
H	3.694320000	3.295385000	1.739691000
C	2.863306000	4.067144000	-0.107541000
H	3.423041000	4.996658000	-0.088531000
C	1.974707000	3.795475000	-1.148724000
H	1.820318000	4.498895000	-1.959105000
C	1.273743000	2.593379000	-1.129551000
H	0.558030000	2.353845000	-1.910440000
Cl	0.106300000	-3.216635000	-0.397912000

$[BiCl_2(py)_5]^+$ (A)

Bi	-0.001137000	-0.000427000	0.000991000
N	2.118430000	1.459571000	-0.000464000
Cl	-0.001885000	-0.003385000	2.696071000
Cl	-0.004060000	-0.000135000	-2.692869000
N	2.043283000	-1.563708000	-0.001190000
N	-2.572545000	0.065973000	0.001890000
N	-0.857814000	-2.426291000	-0.000588000
N	-0.732125000	2.465711000	0.000825000
C	2.453915000	2.175661000	1.086831000
H	1.789542000	2.093370000	1.941717000
C	3.593168000	2.974173000	1.127400000
H	3.827631000	3.534094000	2.025723000
C	4.411832000	3.033685000	-0.001077000
H	5.306437000	3.647999000	-0.001389000
C	4.061345000	2.291261000	-1.129381000
H	4.667503000	2.309195000	-2.028053000

C	2.906716000	1.515150000	-1.088152000
H	2.590588000	0.925028000	-1.943017000
C	2.832636000	-1.654152000	1.083352000
H	2.550385000	-1.045206000	1.936939000
C	3.947091000	-2.486907000	1.123269000
H	4.555793000	-2.530717000	2.019379000
C	4.254458000	-3.251146000	-0.003173000
H	5.117270000	-3.909534000	-0.004055000
C	3.434804000	-3.155366000	-1.128541000
H	3.636699000	-3.730419000	-2.025149000
C	2.337432000	-2.300182000	-1.086800000
H	1.674047000	-2.188590000	-1.939140000
C	-0.691644000	-3.209057000	1.079784000
H	-0.192855000	-2.756164000	1.931310000
C	-1.139919000	-4.526173000	1.118270000
H	-0.987129000	-5.122177000	2.010920000
C	-1.780874000	-5.050253000	-0.005094000
H	-2.140918000	-6.074074000	-0.006940000
C	-1.951405000	-4.236822000	-1.126073000
H	-2.442982000	-4.602797000	-2.020436000
C	-1.476177000	-2.929361000	-1.083203000
H	-1.580903000	-2.260979000	-1.932601000
C	-3.265208000	-0.334870000	1.082143000
H	-2.679742000	-0.672671000	1.931954000
C	-4.656256000	-0.313161000	1.122353000
H	-5.175139000	-0.643446000	2.015147000
C	-5.353216000	0.138214000	0.000874000
H	-6.438093000	0.166229000	0.000543000
C	-4.632905000	0.552835000	-1.120127000
H	-5.133247000	0.910102000	-2.013160000
C	-3.242613000	0.501938000	-1.079115000
H	-2.639881000	0.808830000	-1.928535000
C	-0.535267000	3.235146000	-1.083968000
H	-0.065696000	2.754317000	-1.936856000
C	-0.917136000	4.572981000	-1.124469000
H	-0.741711000	5.156931000	-2.020958000
C	-1.522248000	5.132496000	0.001601000
H	-1.830721000	6.172963000	0.001984000
C	-1.724358000	4.333010000	1.127369000
H	-2.189313000	4.726950000	2.024086000
C	-1.315743000	3.003168000	1.086242000
H	-1.447327000	2.343623000	1.938712000

$[BiCl_2(py)_5]^+$ (B)

Bi	-0.045894000	-0.272182000	-0.503182000
N	0.368573000	-1.674525000	1.776817000

Cl	-0.172639000	0.972953000	-2.769685000
Cl	0.178441000	-2.635563000	-1.691922000
N	2.459394000	-0.533013000	-0.823796000
N	-1.782872000	1.664953000	0.373406000
N	1.280227000	1.931655000	0.374934000
N	-2.462922000	-1.056207000	-0.722832000
C	1.108334000	-2.797244000	1.702757000
H	1.419530000	-3.100560000	0.708276000
C	1.451084000	-3.543020000	2.827856000
H	2.050146000	-4.439861000	2.716803000
C	1.009056000	-3.114434000	4.079609000
H	1.258977000	-3.673903000	4.975297000
C	0.236947000	-1.954694000	4.159931000
H	-0.132813000	-1.585324000	5.109880000
C	-0.058767000	-1.266938000	2.986437000
H	-0.662623000	-0.364636000	3.018538000
C	2.973430000	-0.703259000	-2.054081000
H	2.262721000	-0.725512000	-2.872990000
C	4.340752000	-0.844160000	-2.272655000
H	4.713747000	-0.971992000	-3.282425000
C	5.203168000	-0.819944000	-1.176380000
H	6.273807000	-0.931017000	-1.314226000
C	4.667155000	-0.649697000	0.101000000
H	5.298907000	-0.625312000	0.981605000
C	3.290469000	-0.503552000	0.233204000
H	2.834738000	-0.353645000	1.206123000
C	2.026327000	2.645838000	-0.484957000
H	2.053724000	2.286639000	-1.508844000
C	2.724892000	3.788648000	-0.103187000
H	3.310096000	4.333490000	-0.835540000
C	2.652806000	4.206180000	1.226199000
H	3.186655000	5.091234000	1.557162000
C	1.881118000	3.465901000	2.122582000
H	1.794676000	3.751802000	3.164907000
C	1.210172000	2.339900000	1.652606000
H	0.593079000	1.746741000	2.319868000
C	-1.703896000	2.908750000	-0.128606000
H	-0.971066000	3.062033000	-0.914121000
C	-2.512576000	3.952070000	0.316655000
H	-2.413632000	4.937803000	-0.124198000
C	-3.437969000	3.698683000	1.329516000
H	-4.080600000	4.490109000	1.701793000
C	-3.525650000	2.407780000	1.852322000
H	-4.233139000	2.161671000	2.636310000
C	-2.684064000	1.423198000	1.340763000
H	-2.740964000	0.402456000	1.708198000

C	-2.874319000	-2.135779000	-0.034918000
H	-2.122134000	-2.649979000	0.554722000
C	-4.191170000	-2.583719000	-0.074858000
H	-4.482624000	-3.454663000	0.501129000
C	-5.109535000	-1.894780000	-0.868305000
H	-6.143105000	-2.220836000	-0.923752000
C	-4.677598000	-0.782248000	-1.591402000
H	-5.355956000	-0.221590000	-2.224442000
C	-3.345889000	-0.391829000	-1.487669000
H	-2.964086000	0.470390000	-2.024847000

$[BiCl_2(py)_6]^+$

Bi	0.000000000	0.000000000	0.372469000
N	1.599774000	-1.905489000	-0.345805000
Cl	-2.205007000	-1.513177000	0.841991000
Cl	2.205007000	1.513177000	0.841991000
N	-0.814579000	-1.319830000	-2.231852000
N	-0.855494000	1.214510000	2.467757000
N	0.814579000	1.319830000	-2.231852000
N	0.855494000	-1.214510000	2.467757000
C	1.086619000	-3.146896000	-0.401482000
H	0.053848000	-3.255993000	-0.083685000
C	1.825526000	-4.235485000	-0.854215000
H	1.373337000	-5.220381000	-0.882827000
C	3.142138000	-4.027903000	-1.268889000
H	3.742290000	-4.855829000	-1.632297000
C	3.675248000	-2.739972000	-1.206746000
H	4.694079000	-2.533852000	-1.514777000
C	2.870702000	-1.706026000	-0.734447000
H	3.243114000	-0.689842000	-0.651225000
C	-2.102259000	-1.508321000	-2.560357000
H	-2.824782000	-1.324721000	-1.772434000
C	-2.515668000	-1.933373000	-3.823551000
H	-3.572582000	-2.059945000	-4.032380000
C	-1.547585000	-2.191355000	-4.793303000
H	-1.831541000	-2.525138000	-5.786567000
C	-0.204918000	-2.013015000	-4.457560000
H	0.587421000	-2.202448000	-5.173667000
C	0.109450000	-1.573782000	-3.173668000
H	1.142723000	-1.403084000	-2.891747000
C	-0.109450000	1.573782000	-3.173668000
H	-1.142723000	1.403084000	-2.891747000
C	0.204918000	2.013015000	-4.457560000
H	-0.587421000	2.202448000	-5.173667000
C	1.547585000	2.191355000	-4.793303000
H	1.831541000	2.525138000	-5.786567000

C	2.515668000	1.933373000	-3.823551000
H	3.572582000	2.059945000	-4.032380000
C	2.102259000	1.508321000	-2.560357000
H	2.824782000	1.324721000	-1.772434000
C	-2.176675000	1.338372000	2.692052000
H	-2.835591000	0.903096000	1.951594000
C	-2.688291000	1.968895000	3.821701000
H	-3.761796000	2.041028000	3.954818000
C	-1.800481000	2.492563000	4.761330000
H	-2.168020000	2.989867000	5.653193000
C	-0.431193000	2.361108000	4.532795000
H	0.299480000	2.747852000	5.234173000
C	0.000000000	1.716606000	3.377212000
H	1.054711000	1.597358000	3.160593000
C	2.176675000	-1.338372000	2.692052000
H	2.835591000	-0.903096000	1.951594000
C	2.688291000	-1.968895000	3.821701000
H	3.761796000	-2.041028000	3.954818000
C	1.800481000	-2.492563000	4.761330000
H	2.168020000	-2.989867000	5.653193000
C	0.431193000	-2.361108000	4.532795000
H	-0.299480000	-2.747852000	5.234173000
C	0.000000000	-1.716606000	3.377212000
H	-1.054711000	-1.597358000	3.160593000
C	-1.086619000	3.146896000	-0.401482000
N	-1.599774000	1.905489000	-0.345805000
H	-0.053848000	3.255993000	-0.083685000
C	-1.825526000	4.235485000	-0.854215000
H	-1.373337000	5.220381000	-0.882827000
C	-3.142138000	4.027903000	-1.268889000
H	-3.742290000	4.855829000	-1.632297000
C	-3.675248000	2.739972000	-1.206746000
H	-4.694079000	2.533852000	-1.514777000
C	-2.870702000	1.706026000	-0.734447000
H	-3.243114000	0.689842000	-0.651225000

$[BiCl_2(py)_4][BArF]$

Bi	-5.354731000	-0.511401000	-0.088090000
N	-7.664502000	0.313416000	-0.982071000
Cl	-6.454468000	-0.991570000	2.310838000
Cl	-4.119539000	0.245730000	-2.318597000
N	-5.451515000	1.841023000	0.490745000
N	-4.041422000	-2.800521000	-0.088029000
N	-3.263051000	-0.107465000	1.073389000
C	-8.808006000	0.015837000	-0.338443000
H	-8.710720000	-0.577084000	0.566629000

C	-10.050563000	0.450832000	-0.791161000
H	-10.947204000	0.190022000	-0.240287000
C	-10.108857000	1.221247000	-1.953212000
H	-11.061897000	1.576923000	-2.331463000
C	-8.922522000	1.528157000	-2.621307000
H	-8.922218000	2.124070000	-3.527045000
C	-7.720524000	1.054655000	-2.103468000
H	-6.771862000	1.266860000	-2.588246000
C	-6.456668000	2.319697000	1.250966000
H	-7.196613000	1.602925000	1.586376000
C	-6.532794000	3.661273000	1.603633000
H	-7.357400000	4.006647000	2.216228000
C	-5.536820000	4.534090000	1.161700000
H	-5.570102000	5.585892000	1.426074000
C	-4.497335000	4.032555000	0.379432000
H	-3.695627000	4.662705000	0.015551000
C	-4.490188000	2.680151000	0.060569000
H	-3.707894000	2.253754000	-0.551981000
C	-3.280026000	0.380824000	2.329673000
H	-4.249669000	0.640608000	2.737706000
C	-2.117247000	0.526935000	3.073982000
H	-2.171556000	0.928760000	4.079128000
C	-0.900768000	0.148358000	2.507417000
H	0.018883000	0.253660000	3.066918000
C	-0.889132000	-0.360271000	1.209881000
H	0.033633000	-0.655362000	0.728462000
C	-2.087476000	-0.460146000	0.516252000
H	-2.113070000	-0.821790000	-0.503951000
C	-3.764387000	-3.383550000	1.093763000
H	-4.360347000	-3.057020000	1.941806000
C	-2.752563000	-4.326881000	1.238638000
H	-2.542076000	-4.751823000	2.213203000
C	-2.004443000	-4.687359000	0.116108000
H	-1.188055000	-5.393417000	0.204887000
C	-2.305354000	-4.100805000	-1.112289000
H	-1.740970000	-4.336210000	-2.006989000
C	-3.331296000	-3.161087000	-1.171588000
H	-3.563459000	-2.644768000	-2.097556000
F	1.082657000	-4.419519000	0.316648000
C	2.895866000	-0.765417000	1.158867000
B	3.403478000	0.169151000	-0.097640000
F	2.286902000	-5.182982000	1.958764000
C	2.392788000	-2.060315000	0.914947000
H	2.410439000	-2.452854000	-0.096646000
F	1.299768000	0.441472000	4.986872000
C	1.805334000	-2.392631000	3.245670000

H	1.388839000	-3.005017000	4.036081000
C	1.854290000	-2.853495000	1.927094000
F	0.243258000	-4.546563000	2.326200000
F	1.906126000	-1.473087000	5.829850000
C	2.299548000	-1.120184000	3.511927000
C	2.821211000	-0.319824000	2.486154000
H	3.181026000	0.672550000	2.739679000
F	3.406553000	0.006986000	5.273016000
C	1.369284000	-4.243016000	1.628888000
F	0.437071000	-1.441833000	-4.085343000
F	-1.234519000	-1.719453000	-2.724084000
C	2.232574000	-0.550965000	4.899668000
F	-1.300228000	-0.134170000	-4.215772000
C	2.001809000	0.635580000	-0.819286000
C	1.402600000	-0.145217000	-1.824086000
H	1.925566000	-1.015606000	-2.206020000
F	-1.489880000	2.771108000	0.785612000
C	0.149126000	0.161192000	-2.358345000
F	-1.718737000	3.673906000	-1.176693000
C	-0.564594000	1.273939000	-1.914556000
H	-1.539550000	1.505463000	-2.325024000
F	-0.020141000	4.210348000	0.085925000
C	0.002250000	2.054985000	-0.908735000
F	5.710931000	4.930385000	-1.872062000
C	1.251740000	1.736171000	-0.367898000
H	1.645172000	2.359039000	0.429736000
F	3.837314000	5.396767000	-0.879633000
C	4.344879000	1.427604000	0.372299000
F	8.271527000	2.900552000	2.740089000
C	-0.792043000	3.178717000	-0.312285000
F	6.664470000	2.177865000	4.015188000
C	-0.479494000	-0.769389000	-3.354369000
F	5.727603000	6.026319000	0.006985000
C	4.305081000	2.686350000	-0.249345000
H	3.565609000	2.881294000	-1.019609000
F	7.743841000	0.784485000	2.747105000
C	5.190822000	3.713759000	0.092036000
F	6.125533000	-4.397493000	-0.307521000
C	6.162817000	3.523115000	1.071548000
H	6.845483000	4.318962000	1.341862000
F	7.430824000	-4.277696000	-2.050176000
C	6.235889000	2.274432000	1.689188000
F	7.874963000	-3.113732000	-0.266000000
C	5.351992000	1.251957000	1.338953000
H	5.459470000	0.287720000	1.827044000
F	6.102601000	-1.276605000	-5.570942000

C	7.230568000	2.037045000	2.788648000
F	4.442416000	0.098541000	-5.241051000
C	5.117925000	5.014857000	-0.653952000
F	6.469254000	0.703446000	-4.750125000
C	5.149689000	-1.764978000	-0.718871000
H	5.056646000	-2.140330000	0.295776000
C	4.370465000	-0.671262000	-1.126535000
C	6.194435000	-1.973545000	-2.900511000
H	6.874302000	-2.476413000	-3.576732000
C	6.041281000	-2.406310000	-1.585667000
C	5.435701000	-0.882329000	-3.326498000
C	4.550816000	-0.245240000	-2.454934000
H	3.977070000	0.600014000	-2.824017000
C	6.864580000	-3.547482000	-1.061853000
C	5.610075000	-0.347118000	-4.718692000

Funding

Funding through the FCI, the DFG, and the excellence program LOEWE (LI 2860/3-1, LI 2860/5-1, GRK2112) is gratefully acknowledged.

References

1 J. N. Murphy, F. M. Kerton and L. N. Dawe, *J. Chem. Crystallogr.*, 2014, **44**, 108–114.

2 a) S. L. Benjamin, J. Burt, W. Levason, G. Reid and M. Webster, *J. Fluor. Chem.*, 2012, **135**, 108–113; b) N. Leblanc, M. Allain, N. Mercier and L. Sanguinet, *Cryst. Growth Des.*, 2011, **11**, 2064–2069; c) U. Ensinger, W. Schwarz and A. Schmidt, *Z. Naturforsch. B*, 1982, **37**, 1584–1589; d) H. Preut, F. Huber and G. Alonzo, *Acta Cryst. C*, 1987, **43**, 46–48; e) F. Chen, S. Wang, Y.-H. Li and W. Huang, *J. Chem. Crystallogr.*, 2016, **46**, 309–323; f) I. I. Ozturk, S. K. Hadjikakou, N. Hadjiliadis, N. Kourkoumelis, M. Kubicki, A. J. Tasiopoulos, H. Scleiman, M. M. Barsan, I. S. Butler and J. Balzarini, *Inorg. Chem.*, 2009, **48**, 2233–2245; g) H. J. Breunig, M. Denker and E. Lork, *Z. Anorg. Allg. Chem.*, 1999, **625**, 117–120; h) I. I. Ozturk, S. Yarar, M. Gürgan, D. Ceyhan, C. N. Banti, S. K. Hadjikakou, M. Manoli, E. Moushi and A. J. Tasiopoulos, *Inorg. Chim. Acta*, 2019, **491**, 14–24; i) I. I. Ozturk, S. Yarar, M. Gürgan, D. Ceyhan, N. Panagiotou, A. J. Tasiopoulos, S. Demirkesen and C. Aral, *J. Coord. Chem.*, 2020, **73**, 485–505.

3 a) L. P. Battaglia and A. B. Corradi, *J. Chem. Soc., Dalton Trans.*, 1981, 23–26; b) K. Wójcik, P. Ecorchard, D. Schaarschmidt, T. Rüffer, H. Lang and M. Mehring, *Z. Anorg. Allg. Chem.*, 2012, **638**, 1723–1730; c) L. P. Battaglia and A. B. Corradi, *J. Chem. Soc., Dalton Trans.*, 1983, 2425–2428; d) N. J. Hill, G. Reeske, J. A. Moore and A. H. Cowley, *Dalton Trans.*, 2006, 4838–4844; e) W. Travis, C. E. Knapp, C. N. Savory, A. M. Ganose, P. Kafourou, X. Song, Z. Sharif, J. K. Cockcroft, D. O. Scanlon, H. Bronstein and R. G. Palgrave, *Inorg. Chem.*, 2016, **55**, 3393–3400.

4 M. H. Khan, M. Cai, S. Li, Z. Zhang, J. Zhang, X. Wen, H. Sun, H. Liang and F. Yang, *Eur. J. Med. Chem.*, 2019, **182**, 111616.

5 G. A. Bowmaker, F. M. M. Hannaway, P. C. Junk, A. M. Lee, B. W. Skelton and A. H. White, *Austr. J. Chem.*, 1998, **51**, 325–330.

6 a) I. I. Ozturk, C. N. Banti, S. K. Hadjikakou, N. Panagiotou and A. J. Tasiopoulos, *Inorg. Chim. Acta*, 2019, **497**, 119094; b) D. J. Williams, J. T. Anderton, E. A. Armstrong, M. H. Bowen, R. E. Hart, S. K. Tata, D. R. Smith, K. M. White and D. Vanderveer, *Main Group Chem.*, 2007, **6**, 263–270; c) S. Yarar, I. I. Ozturk, C. N. Banti, N. Panagiotou, C. Papatriantafyllopoulou, M. Manoli, M. J. Manos, A. J. Tasiopoulos and S. K. Hadjikakou, *Inorg. Chim. Acta*, 2018, **471**, 23–33; d) G. R. Willey, L. T. Daly and M. G. B. Drew, *J. Chem. Soc., Dalton Trans.*, 1996, 1063–1067; e) M. Jagenbrein, K. Y. Monakhov and P. Braunstein, *J. Organomet. Chem.*, 2015, **796**, 11–16.

7 a) S. C. James, N. C. Norman and A. Guy Orpen, *J. Chem. Soc., Dalton Trans.*, 1999, 2837–2843; b) N. Shen, J. Li, G. Li, B. Hu, J. Li, T. Liu, L. Gong, F. Huang, Z. Wang and X. Huang, *Inorg. Chem.*, 2019, **58**, 8079–8085; c) F. Li, H.-D. Yin, J. Zhai and D.-Q. Wang, *Acta Cryst. E*, 2006, **62**, m1170-m1172; d) G. A. Bowmaker, F. M. M. Hannaway, P. C. Junk, A. M. Lee, B. W. Skelton and A. H. White, *Austr. J. Chem.*, 1998, **51**, 331–336.

8 M. J. Frisch, G. W. Trucks, H. B. Schlegel, G. E. Scuseria, M. A. Robb, J. R. Cheeseman, G. Scalmani, V. Barone, G. A. Petersson, H. Nakatsuji, X. Li, M. Caricato, A. V. Marenich, J. Bloino, B. G. Janesko, R. Gomperts, B. Mennucci, H. P. Hratchian, J. V. Ortiz, A. F. Izmaylov, J. L. Sonnenberg, D. Williams–Young, F. Ding, F.

Lipparini, F. Egidi, J. Goings, B. Peng, A. Petrone, T. Henderson, D. Ranasinghe, V. G. Zakrzewski, J. Gao, N. Rega, G. Zheng, W. Liang, M. Hada, M. Ehara, K. Toyota, R. Fukuda, J. Hasegawa, M. Ishida, T. Nakajima, Y. Honda, O. Kitao, H. Nakai, T. Vreven, K. Throssell, J. A. Montgomery, Jr., J. E. Peralta, F. Ogliaro, M. J. Bearpark, J. J. Heyd, E. N. Brothers, K. N. Kudin, V. N. Staroverov, T. A. Keith, R. Kobayashi, J. Normand, K. Raghavachari, A. P. Rendell, J. C. Burant, S. S. Iyengar, J. Tomasi, M. Cossi, J. M. Millam, M. Klene, C. Adamo, R. Cammi, J. W. Ochterski, R. L. Martin, K. Morokuma, O. Farkas, J. B. Foresman, D. J. Fox, *Gaussian 16*, Gaussian, Inc., Wallingford CT, 2016.

9 D. Michalska and R. Wysokiński, *Chem. Phys. Lett.*, 2005, **403**, 211–217.

10 P. L. Polavarapu, *J. Phys. Chem.*, 1990, **94**, 8106–8112.

11 E. Denchik, S. C. Nyburg, G. A. Ozin and J. T. Szymanski, *J. Chem. Soc. A*, 1971, 3157–3159.

12 R. P. Oertel and R. A. Plane, *Inorg. Chem.*, 1969, **8**, 1188–1190.

13 A. Kondyurin, N. Byelousova, S. Byelousova and A. Kozulin, *J. Raman Spectrosc.*, 1993, **24**, 825–831.

14 a) D. G. Allis, P. M. Hakey and T. M. Korter, *Chem. Phys. Lett.*, 2008, **463**, 353–356; b) J. Kendrick and A. D. Burnett, *J. Infrared Millim. Terahertz Waves*, 2020, **41**, 382–413.

15 D. F. Hornig, *J. Chem. Phys.*, 1948, **16**, 1063–1076.

16 U. Mayer, V. Gutmann and W. Gerger, *Monatsh. Chem.*, 1975, **106**, 1235–1257.

17 M. A. Beckett, G. C. Strickland, J. R. Holland and K. Sukumar Varma, *Polymer*, 1996, **37**, 4629–4631.

18 J. Ramler and C. Lichtenberg, *Chem. Eur. J.*, 2020, **26**, 10250–10258.

19 a) S. Balasubramaniam, S. Kumar, A. P. Andrews, B. Varghese, E. D. Jemmis and A. Venugopal, *Eur. J. Inorg. Chem.*, 2019, **2019**, 3265–3269; b) J. A. Johnson and A. Venugopal, *J. Chem. Sci.*, 2019, **131**, 114; c) R. Kannan, S. Kumar, A. P. Andrews, E. D. Jemmis and A. Venugopal, *Inorg. Chem.*, 2017, **56**, 9391–9395; d) S. S. Chitnis, A. P. M. Robertson, N. Burford, B. O. Patrick, R. McDonald and M. J. Ferguson, *Chem. Sci.*, 2015, **6**, 6545–6555; e) D. Sharma, S. Balasubramaniam, S. Kumar, E. D. Jemmis and A. Venugopal, *Chem. Commun.*, 2021, **57**, 8889–8892; f) K. Oberdorf, P. Grenzer, N. Wieprecht, J. Ramler, A. Hanft, A. Rempel, A. Stoy, K. Radacki and C. Lichtenberg, *Inorg. Chem.*, 2021, **60**, 19086–19097; g) A. Hanft, K. Radacki and C. Lichtenberg, *Chem. Eur. J.*, 2021, **27**, 6230–6239.

20 J. Ramler, K. Hofmann and C. Lichtenberg, *Inorg. Chem.*, 2020, **59**, 3367–3376.

21 P. Erdmann and L. Greb, *Angew. Chem. Int. Ed.*, 2022, **61**, e202114550.

22 V. Gutmann, *Electrochim. Acta*, 1976, **21**, 661–670.

23 a) U. Beckmann, D. Süslüyan and P. C. Kunz, *Phosphorus Sulfur Silicon Relat. Elem.*, 2011, **186**, 2061–2070; b) I. L. Rusakova and Y. Y. Rusakov, *Magn. Reson. Chem.*, 2020, **58**, 929–940.

24 a) W. Frank, G. J. Reiss and J. Schneider, *Angew. Chem. Int. Ed.*, 1995, **34**, 2416–2417; b) J. Näslund, I. Persson and M. Sandström, *Inorg. Chem.*, 2000, **39**, 4012–4021.

25 a) S. H. Vosko, L. Wilk and M. Nusair, *Can. J. Phys.*, 1980, **58**, 1200–1211; b) C. Lee, W. Yang and R. G. Parr, *Phys. Rev. B*, 1988, **37**, 785–789; c) A. D. Becke, *J. Chem. Phys.*, 1993, **98**, 5648–5652; d) P. J. Stephens, F. J. Devlin, C. F. Chabalowski and M. J. Frisch, *J. Phys. Chem.*, 1994, **98**, 11623–11627.

26 a) R. Ditchfield, W. J. Hehre and J. A. Pople, *J. Chem. Phys.*, 1971, **54**, 724–728; b) W. J. Hehre, R. Ditchfield and J. A. Pople, *J. Chem. Phys.*, 1972, **56**, 2257–2261; c) P. C. Hariharan and J. A. Pople, *Theor. Chim. Acta*, 1973, **28**, 213–222; d) M. M. Francl, W. J. Pietro, W. J. Hehre, J. S. Binkley, M. S. Gordon, D. J. DeFrees and J. A. Pople, *J. Chem. Phys.*, 1982, **77**, 3654–3665; e) M. S. Gordon, J. S. Binkley, J. A. Pople, W. J. Pietro and W. J. Hehre, *J. Am. Chem. Soc.*, 1982, **104**, 2797–2803.
27 W. R. Wadt and P. J. Hay, *J. Chem. Phys.*, 1985, **82**, 284–298.
28 S. Grimme, J. Antony, S. Ehrlich and H. Krieg, *J. Chem. Phys.*, 2010, **132**, 154104.
29 a) M. Cossi, G. Scalmani, N. Rega and V. Barone, *J. Chem. Phys.*, 2002, **117**, 43–54; b) G. Scalmani and M. J. Frisch, *J. Chem. Phys.*, 2010, **132**, 114110.
30 a) C. P. Kelly, C. J. Cramer and D. G. Truhlar, *J. Chem. Theory Comput.*, 2005, **1**, 1133–1152; b) M. Sparta, C. Riplinger and F. Neese, *J. Chem. Theory Comput.*, 2014, **10**, 1099–1108.
31 T. Lu and F. Chen, *J. Comput. Chem.*, 2012, **33**, 580–592.